

AD \_\_\_\_\_

Award Number: DAMD17-00-1-0476

TITLE: Identification of Structural Domains of ESX Required for  
Breast Cell Transformation

PRINCIPAL INVESTIGATOR: Arthur Gutierrez-Hartmann, M.D.

CONTRACTING ORGANIZATION: University of Colorado  
Health Science Center  
Denver, Colorado 80045-6508

REPORT DATE: June 2002

TYPE OF REPORT: Annual

PREPARED FOR: U.S. Army Medical Research and Materiel Command  
Fort Detrick, Maryland 21702-5012

DISTRIBUTION STATEMENT: Approved for Public Release;  
Distribution Unlimited

The views, opinions and/or findings contained in this report are those of the author(s) and should not be construed as an official Department of the Army position, policy or decision unless so designated by other documentation.

20021105 028

REPORT DOCUMENTATION PAGE			Form Approved OMB No. 074-0188	
Public reporting burden for this collection of information is estimated to average 1 hour per response, including the time for reviewing instructions, searching existing data sources, gathering and maintaining the data needed, and completing and reviewing this collection of information. Send comments regarding this burden estimate or any other aspect of this collection of information, including suggestions for reducing this burden to Washington Headquarters Services, Directorate for Information Operations and Reports, 1215 Jefferson Davis Highway, Suite 1204, Arlington, VA 22202-4302, and to the Office of Management and Budget, Paperwork Reduction Project (0704-0188), Washington, DC 20503				
1. AGENCY USE ONLY (Leave blank)	2. REPORT DATE June 2002	3. REPORT TYPE AND DATES COVERED Annual (1 June 2001 - 31 May 2002)		
4. TITLE AND SUBTITLE Identification of Structural Domains of ESX Required for Breast Cell Transformation		5. FUNDING NUMNUMBER DAMD17-00-1-0476		
6. AUTHOR(S) Arthur Gutierrez-Hartmann, M.D.				
7. PERFORMING ORGANIZATION NAME(S) AND ADDRESS(ES) University of Colorado Health Science Center Denver, Colorado 80045-6508 email - a.gutierrez-hartmann@UCHSC.edu		8. PERFORMING ORGANIZATION REPORT NUMBER		
9. SPONSORING / MONITORING AGENCY NAME(S) AND ADDRESS(ES) U.S. Army Medical Research and Materiel Command Fort Detrick, Maryland 21702-5012		10. SPONSORING / MONITORING AGENCY REPORT NUMBER		
11. SUPPLEMENTARY NOTES Report contains color				
12a. DISTRIBUTION / AVAILABILITY STATEMENT Approved for Public Release; Distribution Unlimited			12b. DISTRIBUTION CODE	
13. ABSTRACT (Maximum 200 Words) ESX encodes an Ets family transcription factor gene that is potentially important in breast cancer because the ESX genomic region (chromosome 1q32.1) is amplified in 50% of early breast cancers and ESX mRNA is over-expressed in human breast ductal carcinoma in situ (DCIS). However, the precise molecular mechanism by which ESX mediates breast cell transformation remains unknown. We have previously shown that the non-transformed MCF-12A cell line fails to express ESX, while the transformed T47D breast cancer cell line does express ESX. When we enforce ESX expression in MCF-12A cells, they display a transformed phenotype, whereas abrogation of endogenous ESX expression in T47D cells results in a marked reduction of T47D colony formation. We generated a GFP-ESX fusion to determine its subcellular localization, via confocal microscopy, in MCF-12A cells stably expressing GFP-ESX. To our surprise, we found that GFP-ESX is initially expressed in the nucleus and then stably appears in the peri-nuclear cytoplasmic region. Since these GFP-ESX stable cell lines also display the transformed phenotype, the question arises as to how a putative transcription factor residing in the cytoplasm mediates cellular transformation? Supporting this notion is that immuno-histochemical analysis of primary human breast cancer specimens and T47D cells, also show that ESX localization is primarily cytoplasmic. These data indicate that ESX functions primarily via cytoplasmic mechanisms.				
14. SUBJECT TERMS breast cancer, Ets, ESX, HER2, neu, ErbB2, transformation, transcription			15. NUMBER OF PAGES 58	
			16. PRICE CODE	
17. SECURITY CLASSIFICATION OF REPORT Unclassified	18. SECURITY CLASSIFICATION OF THIS PAGE Unclassified	19. SECURITY CLASSIFICATION OF ABSTRACT Unclassified	20. LIMITATION OF ABSTRACT Unlimited	

## Table of Contents

Cover.....	1
SF 298.....	2
Table of Contents.....	3
Introduction.....	4
Body.....	4
Key Research Accomplishments.....	7
Reportable Outcomes.....	7
Conclusions.....	8
References.....	8
Appendices.....	9

## INTRODUCTION

The Ets family of transcription factors contains several members that are important components of the cellular pathways leading to tumorigenesis (1). For example, several Ets members are downstream targets of oncogenic Ras (2); dominant-negative Ets reverses the transformed phenotype (3,4); and, Ets proteins have been shown to regulate a repertoire of genes that govern cellular survival, proliferation and migration (1,6). Moreover, several Ets factors have been implicated in breast cancer (1,6). However, the ability of Ets factors to transform human breast cells, the identity of the precise Ets factor required for breast cell transformation, and the molecular mechanism by which such an Ets factor mediates breast cell transformation, all remain unknown. The ESX gene is an Ets member that is particularly relevant to breast cancer. ESX is located on chromosome 1q32.1, in a region that is amplified in 50% of early breast cancers. ESX mRNA is over-expressed in human breast ductal carcinoma in situ (DCIS) (7-9). Also, there is a positive feedback loop between the HER2/neu proto-oncogene and ESX, in that HER2/neu activation induces ESX expression, while ESX activates the HER2/neu promoter via a putative ESX DNA binding site (7-9). Finally, HER2/neu and ESX expression levels are positively correlated in human breast cancer cell lines (7-9). Based on these observations, we have chosen to determine whether ESX is capable of transforming immortalized, but non-transformed MCF-12A human breast cells, and to determine the precise mechanism(s) by which ESX transforms these human breast epithelial cells.

## BODY

**Task 1:** To define the modular structural domains of ESX ( $\pm$  DNA) using Cleveland and peptide sequencing analysis.

We have made continued progress towards accomplishing this aim. As noted in our previous Progress Report, we have fully characterized an HA-tagged ESX mammalian expression construct, showing that HA-ESX is expressed as a protein of about ~47 kDa in transiently transfected HeLa and MCF-12A cells. We also characterized the transcription potency and promoter specificity of HA-ESX. Taken together, these data revealed that HA-ESX differentially regulates several breast-cancer relevant gene promoters, in particular collagenase and HER2/neu.

We also generated ESX as a fusion protein with GST, and we have optimized conditions to express recombinant GST-ESX in bacteria and to purify it to homogeneity. Having made GST-ESX containing a thrombin cleavage site between GST and ESX, we also have been optimizing conditions for cleavage of ESX from GST-ESX immobilized on glutathione beads. While this approach has been releasing intact ESX, the amounts released were initially very low (~2-5% of total). We have now optimized the expression and purification of ESX devoid of the GST leader in an efficient manner. We have initiated the Cleveland digestion protocol, as originally described in our proposal.

Using this highly purified recombinant GST-ESX, we generated rabbit polyclonal anti-ESX antibodies, in collaboration with ABR, Inc., in Golden, CO, as originally proposed. These antibodies, which are very important reagents, are now commercially sold by ABR to the

entire scientific community, thus providing an invaluable research tool to all breast cancer investigators. We have characterized these anti-ESX antibodies and shown that they recognize a ~47 kDa nuclear protein that is expressed in T47D breast cancer cells. Importantly, we also documented that ESX is not expressed in the non-transformed human MCF-12A mammary cell line. Additionally, these anti-ESX antibodies have already been very useful in measuring ESX protein expression levels in the transcription and transformation assays, as described above. We also initiated a new project with these anti-ESX antibodies and we have optimized the chromatin immunoprecipitation (ChIP) assay to show that ESX actually binds to certain cellular target genes in vivo, during the initial stages of ESX expression.

In the past year, we have used these anti-ESX antibodies in immuno-histochemical (IHC) analysis of ESX expression in primary human breast cancer specimens and immuno-cytochemical (ICC) analysis of T47D (ESX<sup>+</sup>), MCF-12A (ESX<sup>-</sup>) and MCF-12A (ESX<sup>+</sup>) human mammary cell lines. We have performed these pilot studies in collaboration with Dr. Menakshi Singh, in our Pathology Dept., and the data show that endogenous ESX is primarily located in the cytoplasm in the primary human breast cancer specimens and the T47D breast cancer cell lines. By contrast, no ESX protein was detected in the control MCF-12A cells, whereas ESX was detected primarily localized to the nucleus in MCF-12A cells transiently transfected with an HA-ESX expression vector. These data suggested differential localization of ESX in malignant (cytoplasmic) cell lines and tissues vs nonmalignant (nuclear) cell lines.

Since we had not been able to detect HA-ESX in the MCF-12A cells stably transfected with the HA-ESX expression vector, we were unable to determine its subcellular localization, despite the fact that HA-ESX actually transformed these human mammary cells. However, the cytoplasmic localization of ESX in the T47D breast cancer cell lines and primary tissues forced us to re-consider our original hypothesis and also forced us to more carefully analyze the subcellular localization of ESX. To this end, we constructed a GFP-ESX fusion and generated two pools of MCF-12A cells stably expressing this construct. Real-time GFP-ESX expression in living cells was followed on a daily basis using fluorescence microscopy during the G418 selection process. These studies revealed that GFP-ESX is initially robustly expressed in the nucleus in most cells, and in the cytoplasm in fewer cells. After about 28-30 hours, the cells expressing GFP-ESX in the nucleus appear to die off, and the population expressing GFP-ESX in the cytoplasm persist and become the dominant population. We are testing these GFP-ESX-expressing stable pools to determine whether they too are transformed, as our initial HA-ESX stable pools.

**Task 2:** To define the modular domain of ESX required for breast cell transformation.

We have made the most significant progress in this aim and have made several important discoveries about the role of ESX in breast epithelial cell proliferation and transformation. First of all, we have completed the preliminary studies showing that transient expression of HA-ESX and HA-VP16-ESX in MCF-12A cells results in increased colony formation and these data are part of a manuscript submitted to DNA and Cell Biology. (A draft of this Ms was previously submitted in the Appendix of the previous Progress Report). Using a colony

formation assay, we found that HA-ESX and HA-Ets-2 mediated MCF-12A cell colony formation rates that approached those generated by oncogenic V12 Ras, whereas empty vector had a negligible effect. By contrast, in immortalized and transformed T47D breast cancer cells, which express abundant amounts of HER2/neu and ESX, we found that anti-sense and dominant-negative HA-ESX inhibited T47D colony formation, whereas control vector allowed formation of many colonies.

As noted above, we have also established a number of MCF-12A cell lines stably expressing either vector control HA-ESX, HA-VP16-ESX, HA-ETS-2, or V12-Ras. We chose the MCF-12A cell line because it is immortalized, but nontransformed, and importantly these cells fail to express endogenous ESX protein. We used pCGN2-HA-Ets-2 and pSVRas expression vectors as positive controls for transformation. Stable expression of ESX induced EGF-independent proliferation, serum-independent MAPK phosphorylation and growth in soft agar. Additionally, stable ESX expression conferred increased cell adhesion, motility and invasion in two-dimensional and trans-well filter assays. An epithelial to mesenchymal morphological transition was noted in stable ESX cells. In three-dimensional cultures, parental and control (pCGN2) cells formed highly organized duct-like structures with evidence of cell polarity, ECM adhesion-dependent proliferation and cell survival, and lack of cellular invasion into surrounding matrix. Remarkably, the ESX stable cells formed solid, disorganized structures, with lack of cell polarity and loss of dependence on ECM adhesion for cell proliferation and survival. In addition, ESX cells invaded the surrounding matrix, indicative of a transformed and metastatic phenotype. The positive control cell lines, HA-Ets-2 and V12Ras, also increased adhesion, motility and invasion, while displaying differences in cellular morphology. Finally, the negative control (pCGN2) cells lacked any evidence of the transformed and EMT phenotypes.

These studies have been completed in collaboration with Dr. Pepper Schedin of the AMC Cancer Center here in Denver, and we have submitted the Ms. detailing these results to Molecular & Cellular Biology (see Appendix). This study establishes ESX and Ets-2 as putative oncogenes capable of conferring the transformed phenotype to otherwise normal MCF-12A human mammary epithelial cells. We have also established 2 pools of stable MCF-12A cell lines expressing GFP-ESX, and the transformed phenotype is currently being determined in these cells. Moreover, we have initiated our "domain" deletion studies to determine which domain of ESX is required for cytoplasmic vs nuclear localization and for transformation. Thus, we plan to complete an exhaustive structure-function analysis of ESX. We have generated an exon 7 deletion (GFP-ESX $\Delta$ 7) construct, which retains the transcription activation domain (TAD), the serine-rich box and the DNA binding domain (DBD), but it is devoid of the HMG domain and of the putative nuclear localization signal (NLS). Preliminary studies reveal that indeed GFP-ESX $\Delta$ 7 is visualized only in the cytoplasm at all time points after transfection, and thus we have removed the NLS. We are anxious to determine the transcription and transforming capabilities of this construct. Finally, we are in the process of making the remaining panel of ESX internal-deletion mutants, each fused to GFP. Each of these mutants will be tested for their ability to activate target the Her2/Neu target promoter, and for their ability to transform MCF-12A cells.

**Task 3:** To identify the proteins that associate with the ESX transforming domain using MALDI-TOF.

As noted above, our more recent discovery that endogenous ESX is localized primarily to the cytoplasm in human breast cancer specimens and in the T47D breast cancer cell line, we have had to reassess our original hypothesis. We originally hypothesized that ESX main function was as a transcription factor, however, it has now become clear that it functions primarily in the cytoplasm. The GFP-ESX $\Delta$ 7 construct will allow us to exclude any nuclear residence requirements for ESX function, since this construct fails to enter the nucleus. Despite this change in the sub-cellular site of ESX action, nevertheless, it remains clear that ESX transforms MCF-12A cells. Thus, the overall approach to this Aim remains essentially unchanged. IN this regard, we have already generated an ESX construct that contains the Tandem Affinity Peptide (TAP) tag fused to its amino-terminus, and established MCF-12A cells that stably express this construct. Our plan is to use two sequential affinity chromatography steps in order to purify the ESX protein complex, to then separate the proteins in the complex using SDS-PAGE, and to cut out the protein bands and submit them to MALDI-TOF mass spectrometry for identification. We would complete the same analysis with ESX internal deletion mutant(s) that fail to transform MCF-12A cells, and look for proteins that are missing in that complex compared to the wild-type Esx complex.

#### KEY RESEARCH ACCOMPLISHMENTS

- ◆ Establishment of pools of MCF-12A cells stably expressing HA-ESX, HA-VP16-ESX, HA-Ets2, V12-Ras or vector control.
- ◆ Documenting that ESX and Ets-2 function as oncogenes and transform MCF-12A human mammary cells.
- ◆ Showing that endogenous ESX is localized to the cytoplasm in human breast cancer specimens and T47D breast cancer cell lines, using IHC and ICC, respectively.
- ◆ Establishment of GFP-ESX stable pools in MCF-12A cells and discovering that GFP-ESX is primarily localized to the peri-nuclear cytoplasmic subcellular region.
- ◆ Generating a GFP-ESX $\Delta$ 7 construct, whose expression fails to show any nuclear component during any phase of temporal expression.

#### REPORTABLE OUTCOMES

##### Abstracts:

- (1) Identification of ESX-Regulated Genes that Promote Breast Cell Transformation by cDNA Microarray Analysis, G.J. Cappelletta, Kristin Eckel, Arthur Gutierrez-Hartmann, University of Colorado Health Sciences Center, Denver, CO. National Endocrine Society Meeting, Denver, CO, June, 2001.
- (2) Analysis of ESX Function in the Development of Human Breast Cancer. J.D. Prescott, A. Gutierrez-Hartmann, University of Colorado Health Sciences, Denver, CO. National Endocrine Society Meeting, Denver, CO, June, 2001.
- (3) The ESX Transcription Factor in Human Breast Cancer: Localization of the ESX Protein in Human Breast Epithelial Cells and Identification of Her-2 as an ESX Target Gene. J.D. Prescott, M. Singh, A. Gutierrez-Hartmann, University of Colorado Health

Sciences, Denver, CO. National Endocrine Society Meeting, San Francisco, CA, June, 2002.

- (4) ESX induces transformation and functional epithelial to mesenchymal transition in MCF-12A mammary epithelial cells. P.J. Schedin, K.L. Eckel, S.M. McDaniel, K.S. Brodsky, J.J. Tentler, A. Gutierrez-Hartmann, AMC Cancer Research Center, Denver, CO; University of Colorado Health Sciences Center, Denver, CO. American Association for Cancer Research Meeting, San Francisco, CA, 2002.
- (5) The Ets Transcription Factor ESX Directly Activates Expression of the HER-2 Proto-oncogene. J.D. Prescott & A. Gutierrez-Hartmann, University of Colorado Health Sciences, Denver, CO. San Antonio Breast Cancer Symposium Abstract, 2002

#### Manuscripts

- (1) K.L. Eckel, J.T. Tentler, G.J. Cappetta, S.E. Diamond and A. Gutierrez-Hartmann. (2001) The epithelial-specific ETS transcription factor ESX/ESE-1/Elf-3 modulates malignancy-associated gene expression and breast cell growth. DNA & Cell Biol., under review.
- (2) P.J. Schedin, K.L. Eckel, S.M. McDaniel, K.S. Brodsky, J.J. Tentler and A. Gutierrez-Hartmann. ESX Induces Transformation and Functional Epithelial to Mesenchymal Transition in MCF-12A Mammary Epithelial Cells. Mol. Cell. Biol., submitted.

#### Reagents Developed

- (1) Rabbit polyclonal anti-ESX antibodies now commercialized by ABR, Inc., Golden, CO.

#### Funding applied for and received based on this work

- (1) J.D. Prescott, National DOD Pre-doctoral Award, 6/2001: Awarded, 6/2002.

### **CONCLUSIONS**

The data that we have generated thus far are of particular significance to breast cancer because we have shown that ESX regulates expression of the HER2/neu promoter and mediates transformation of MCF-12A human breast cells. Moreover, using the anti-ESX antibody that we generated in collaboration with ABR, Inc, we have shown that the non-transformed MCF-12A cells fail to express ESX, while the transformed and malignant T47D breast cancer cells express abundant amounts of ESX. Recent IHC and ICC data reveal that endogenous ESX is expressed in the cytoplasm in human breast cancer specimens and in T47D breast cancer cells, and that stably expressed GF-ESX is also expressed in the cytoplasm in MCF-12A cells. These data raise questions as to how a transcription factor mediates its effects as a cytoplasmically-localized protein, and whether such cytoplasmic localization is required for its oncogene effects. Given that endogenous ESX is expressed cytoplasmically in human breast cancer, these issues become very relevant. Ultimately, we anticipate that these studies will provide a novel marker and several new drug targets to use in our battle against breast cancer.

### **REFERENCES**

1. Wasylyk, B, and Nordheim, A. 1997. Ets transcription factors: Partners in the integration of signal responses., p. 251-284. In A. Papavassiliou (ed.), Transcription Factors in Eukaryotes. Landes Bioscience.

2. Wasylyk, B, Hagman, J, and Gutierrez-Hartmann, A. 1998. Ets transcription factors: nuclear effectors of the Ras/MAP kinase signaling pathway. *Trends Biochem. Sci.* 23:213-216.
3. Sapi, E, Flick, M, Rodov, S, and Kacinski, B. 1998. Ets-2 transdominant mutant abolishes anchorage-independent growth and anchorage-stimulating factor-stimulated invasion by BT20 breast carcinoma cells. *Cancer Res.* 58:1027-1033.
4. Delannoy-Courdent, A, Mattot, V, Fafeur, V, Fauquette, W, Pollet, I, Calmels, T, Vercamer, C, Boilly, B, Vandebunder, B, and Desbiens, X. 1998. The expression of Ets-1 transcription factor lacking its activation domain decreases uPA proteolytic activity and cell motility, and impairs normal tubulogenesis and cancerous scattering in mammary epithelial cells. *J. Cell Sci.* 111:1521-1534.
5. Galang, C, Garcia-Ramirez, J, Solski, P, Westwick, J, Der, C, Neznanov, N, Oshima, R, and Hauser, C. 1996. Oncogenic Neu/ErbB-2 increases, Ets, AP-1 and NF-kB-dependent gene expression, and inhibiting Ets activation blocks Neu-mediated cellular transformation. *J. Biol. Chem.* 271:7992-7998.
6. Janknecht, R, and Nordheim, A. 1993. Gene regulation by Ets proteins. *Biochim. Biophys. Acta* 1155:346-356.
7. Chang, C, Scott, G, Kuo, W, Xiong, X, Suzdaltseva, Y, Park, J, Sayre, P, Erny, K, Collins, C, Gray, J, and Benz, C. 1997. ESX: A structurally unique Ets overexpressed early during human breast tumorigenesis. *Oncogene* 14:1617-1622.
8. Oettgen, P, Alani, R, Barcinski, M, Brown, L, Akbarali, Y, Boltax, J, Kunsch, C, Munger, K, and Libermann, T. 1997. Isolation and characterization of a novel epithelium-specific transcription factor, ESE-1, a member of the ets family. *Mol. Cell. Biol.* 17:4419-4433.
9. Tymms, M, Ng, A, Thomas, R, Schutte, B, Zhou, J, eyre, H, Sutherland, G, Seth, A, Rosenberg, M, Papas, T, Debouck, C, and Kola, I. 1997. A novel epithelial-expressed ETS gene, ELF3: Human and murine cDNA sequences, murine genomic organization, human mapping to 1q.32.2 and expression in tissues and cancer. *Oncogene* 15:2449-2462.

## APPENDICES

Enclosed is a draft of our second Ms., that has been submitted to Molecular & Cellular Biology. It is a total of 63 pages.

P.J. Schedin, K.L. Eckel, S.M. McDaniel, K.S. Brodsky, J.J. Tentler and A. Gutierrez-Hartmann. ESX Induces Transformation and Functional Epithelial to Mesenchymal Transition in MCF-12A Mammary Epithelial Cells. Mol. Cell. Biol., submitted.

# **ESX Induces Transformation and Functional Epithelial to Mesenchymal Transition in MCF-12A Mammary Epithelial Cells**

Pepper J. Schedin, Kristin L. Eckel, Shauntae M. McDaniel, Kelley S. Brodsky,

John J. Tentler and Arthur Gutierrez-Hartmann\*

Departments of Medicine and of Biochemistry & Molecular Genetics, Program in Molecular  
Biology, and Colorado Cancer Center, University of Colorado Health Sciences Center

\*To whom correspondence should be addressed: University of Colorado Health Sciences Center,  
4200 East Ninth Avenue Box B-151, Denver, CO 80262

**Telephone:** 303-315-8443

**FAX:** 303-315-4525

**Email:** [a.gutierrez-hartmann@uchsc.edu](mailto:a.gutierrez-hartmann@uchsc.edu)

**Running Title:**

## Abstract

ESX is an epithelial-restricted member of a large family of transcription factors known as the Ets family. ESX expression has been shown to be correlated with Her2/neu proto-oncogene amplification in highly-aggressive breast cancers and induced by Her2/neu in breast cell lines, but its role in tumorigenesis is unknown. Previously we have shown that ESX enhances breast cell survival in colony formation assays. In order to determine whether ESX can act as a transforming gene, we stably transfected MCF-12A human epithelial mammary cells with the pCGN2-HA-ESX expression vector. The MCF-12A cell line is immortalized, but nontransformed, and importantly, these cells fail to express endogenous ESX protein. We used pCGN2-HA-Ets-2 and pSVRas expression vectors as positive controls for transformation. Stable expression of ESX induced EGF-independent proliferation, serum-independent MAPK phosphorylation and growth in soft agar. Additionally, stable ESX expression conferred increased cell adhesion, motility and invasion in two-dimensional and trans-well filter assays, and an epithelial to mesenchymal morphological transition. In three-dimensional cultures, parental and control (pCGN2) cells formed highly organized duct-like structures with evidence of cell polarity, ECM adhesion-dependent proliferation and cell survival, and lack of cellular invasion into surrounding matrix. Remarkably, the ESX stable cells formed solid, disorganized structures, with lack of cell polarity and loss of dependence on ECM adhesion for cell proliferation and survival. In addition, ESX cells invaded the surrounding matrix, indicative of a transformed and metastatic phenotype. Taken together, these data show that ESX expression alone confers a transformed and in vitro metastatic phenotype to otherwise normal MCF-12 cells.

## Introduction

The ETS family is a large group of transcription factors that are known to play significant roles in development, differentiation, and transformation [Graves, 1998 #318; Wasylyk, 1998 #948]. ETS family members are defined by the ETS domain, a highly-conserved, 85 amino acid DNA-binding domain (DBD) that is folded into a novel winged helix-turn-helix DNA-binding motif [Donaldson, 1994 #208; Donaldson, 1996 #209]. ESX, also known as ESE-1, Ert, Jen and Elf-3, is unique among ETS members with regards to its expression and its structure. Specifically, its expression is restricted to epithelial cells and the protein contains two additional motifs, a serine-rich box and an AT-hook domain [Chang, 1997 #135; Chang, 1999 #136; Benz, 1997 #63; Oettgen, 1997 #666]. The founding member of the ETS family, the *v-ets* oncogene in the E26 retrovirus, causes hematopoietic malignancies in chickens [Leprince, 1983 #508]. An important aspect of this family of transcription factors is that several ETS members have also been identified as critical components of the cellular pathways leading to tumorigenesis in humans [Dittmer, 1998 #204; Wasylyk, 1998 #948].

Several different lines of evidence suggest that ETS factors play a particularly relevant role in breast cancer. For example, ETS factor over-expression has been reported in human and rodent mammary tumor biopsies and cell lines, including members of the ETS-1, PEA-3 and ESX subfamilies [Baert, 1997 #44; Benz, 1997 #63; Gilles, 1997 #295; Watabe, 1998 #949][Dittmer, 1998 #204][Shepherd, 2000 #826]. Moreover, expression of dominant-negative (dn) Ets DBD constructs has been shown to completely block the anchorage-independent growth and cellular invasiveness of MMT and BT20 breast carcinoma cell lines [Sapi, 1998 #783; Delannoy-Courdent, 1998 #192]. These results provide compelling data supporting a direct role

of ETS proteins in transformation of mammary epithelial cells. Of these various ETS factors, ESX has been recently implicated as a key transcription factor associated with human breast cancer [Tymms, 1997 #912; Chang, 1997 #135; Liu, 1992 #529]. For example, ESX has been shown to be amplified in ~50% of early breast tumors [Tymms, 1997 #912] and ESX expression is significantly increased in ductal carcinoma in situ (DCIS) [Chang, 1997 #135; Liu, 1992 #529]. Furthermore, there is a positive correlation between ESX and HER2/neu proto-oncogene expression in human breast cancers, and this co-expression strongly correlates with a highly metastatic phenotype and poor prognosis [Benz, 1997 #63; Chang, 1997 #135; Liu, 1992 #529]. A positive-feedback-regulatory loop between HER2/neu and ESX has been suggested by the demonstration that HER2/neu activation induced ESX expression while the Her2/neu promoter can be activated by ESX via an ETS-like DNA sequence motif [Eckel, 2001 #1006; O'Hagan, 1998 #660; Benz, 1997 #63]. While these studies clearly implicate ETS factors in breast cancer, the ability of any specific ETS factor, including ESX, to actually transform normal breast cells has not been shown.

To investigate the potential roles of ESX in breast cell transformation and acquisition of metastatic potential, we generated stable transfectants of MCF-12A human mammary epithelial cells expressing ESX, Ets-2 and V12-Ras. We chose MCF-12A cells as the model system, since these cells are immortalized, but nontransformed human mammary epithelial cells [Paine, 1992 #685] that fail to express ESX (see below). In this paper, we focused on functional assays that measure cellular transformation and metastatic potential, with particular emphasis on examining the epithelial-to-mesenchymal transition (EMT). The rationale for this emphasis is that EMT has been strongly correlated with multiple events in the metastatic cascade, including the ability of tumor

cells to disseminate from the primary tumor, to intravasate into vasculature or lymphatics, and to extravasate into tissue at secondary sites [Kantor, 1996 #1018][Horwitz, 1995 #1017; Hay, 1995 #1016]. At the cellular level, EMT involves loss of epithelial characteristics, such as apical-basal cell polarity and cell-cell adhesion junctions, and gain of mesenchymal characteristics, such as motility and invasiveness; all attributes that are readily measurable in vitro [Kantor, 1996 #1018]. In this paper we show that stable expression of ESX is sufficient to confer a transformed and in vitro metastatic phenotype to otherwise normal, but immortalized MCF-12 cells, suggesting that ESX may be a critical downstream effector of the HER2/neu pathway.

## Materials and Methods

*Plasmid Constructs-* A cDNA spanning the coding sequence of human ESX mRNA was amplified by RT-PCR, as previously described, and subcloned into pCR2.1 (Invitrogen Corporation). The ESX cDNA sequence and its orientation was verified by dideoxy sequencing by the UCHSC Cancer Center DNA Sequencing Core facility. ESX was excised from pCR2.1-ESX by digestion with Bgl II and Afl III, and the 1116 base pair Bgl II ESX fragment was ligated into a BamH I linearized and dephosphorylated pCGN2-HA vector to generate pCGN2-HA-ESX (Bradford, Brodsky et al. 2000). The plasmid pCGN-HA-Ets-2 was provided by Dr. Michael Ostrowski (Ohio State University).

*Cell line culture conditions-* MCF-12A cells were obtained from ATCC (Manassas, VA). For routine maintenance, cells were grown in complete media consisting of Ham's F12/Dulbecco modified Eagle media (DME) containing 100 ng/ml cholera toxin (Gibco/BRL), 0.5 µg/ml hydrocortisone (Sigma), 10 µg/ml insulin (Sigma), 20 ng/ml EGF (Sigma), and 5% horse serum (Gibco/BRL). *Stable Cell Lines-* Immortalized but not transformed MCF-12A human mammary epithelial cells were transfected by electroporation with 2 µg of pRSVneo and either 20 µg of control pCGN2 vector, pCGN2-HA-ESX, pCGN2-HA-Ets-2 or pSV-Ras (oncogenic V12-Ras). Following electroporation, cells were immediately plated into 60 mm dishes with 3 ml of complete media, as described above. After a 24 hour incubation in 95% O<sub>2</sub> and 5% CO<sub>2</sub> at 37° C, media was replaced with fresh Ham's F12/DME containing all of the supplements listed above, as well as 500 µg/ml G418 in order to select for geneticin-resistant cells. After two weeks of selection, pools of G418-resistant cells, denoted as pCGN2-P, ESX-P, Ets-2-P, and V12Ras-P,

were re-plated, expanded and maintained in complete media containing 200 µg/ml G418. For experiments described, log phase cells between passages 4-10 were utilized.

*Western Blot Analysis*- Media was removed from stable populations of MCF-12A cells that had been transfected with pCGN2 (empty vector), pCGN2-HA-ESX, pCGN2-HA-Ets-2, or pSV-Ras. Cells were rinsed on the plate with 1 X PBS and harvested with 1 X PBS with 3mM EDTA. The cell pellet was rinsed in 1 X PBS containing 0.1% protease inhibitor mix (PIM) (Boehringer) and spun. The resulting cell pellet was resuspended in 100 µl lysis buffer consisting of 0.1 M  $\text{KHPO}_4$ , 1 mM DTT, and 0.1% PIM. Three freeze/thaw cycles were performed and cellular debris was removed by a 10-minute centrifugation at 13,000 g. The supernatant protein was measured by Bradford assay. Equal protein was loaded onto a 10% SDS polyacrylamide gel and analysed by Western blot. Protein from the polyacrylamide gel was transferred onto a nitrocellulose membrane and the membrane was incubated in 5% milk and 0.2% Tween 20 in 1 X PBS (blocking buffer). The membrane was probed for sixteen hours with a polyclonal anti-ESX antibody (Affinity Bioreagents, Golden, CO) at a dilution of 1:1,000 in blocking buffer at 4°C. A goat-anti-rabbit-HRP antibody (Santa Cruz Biotechnology) at a dilution of 1:5,000 in blocking buffer was used to probe membranes. Protein bands were visualized by using enhanced chemiluminescence (ECL) (Amersham Pharmacia Biotech), according to manufacturer's protocol.

*Phospho-MAP Kinase Assays*- Stable cell lines were starved for sixteen hours in media containing 0.1% serum and no EGF. Cells were then harvested by lysis directly on the plate with 2 X SDS protein load dye (Owl Separation Systems) consisting of 0.25 M Tris/HCl pH 6.8, 2% SDS, 10% β-mercaptoethanol, 30% glycerol, and 0.01% bromophenol blue. Lysates were sheered with a 25G needle and boiled for five minutes before loading onto a 10% SDS

polyacrylamide gel and analysed with a phospho-p44/42 MAP kinase antibody (New England Biolabs) by Western blot, performed as described above.

*Cell Growth Assay*- Cells were harvested from sub-confluent plates and were resuspended in complete media and plated in 24 well plates at a density of 10,000 cells per well. After 24 hours, cells were harvested from the first plate and counted on a hemocytometer. Media was changed on the remaining cells to F12/DME with reduced serum (1%) and no EGF, or media with reduced serum (1% ) and the addition of 20 ng/ml EGF. This restricted media was replaced on cells every 24 hours in order to prevent growth factor accumulation from neighboring cells. Cells were harvested every 24 hours for 5 days and cell number determined.

*Soft Agar Assay*- Stable pools were harvested at 80-90% confluency and counted. A base layer of 0.35% low melting point agarose (SeaPlaque) in 1X DME (Gibco/BRL) and 10 % horse serum (Gibco/BRL) was poured into 60 mm plates and allowed to harden at 4°C. Twenty thousand cells of each stable cell line were resuspended in complete media plus agar mixture at 42°C and seeded on top of the solidified base layer. Plates were incubated at 37°C in 95% O<sub>2</sub> and 5% CO<sub>2</sub> for 4 weeks. Plates were fed drop-wise with complete media as needed, to keep the agar mixture from drying out. After four weeks, plates were photographed at 40X for maximal colony visibility.

*Adhesion Assay* – Log phase cells were harvested with trypsin-EDTA and re-suspended at 60,000 cells per well in 96 well tissue culture plates (Nunc) in complete medium supplemented with G418 (200 µg/ml). After 30, 45, 60, and 75 minutes of 37° C incubation, cells were rinsed 3X with Hank's Buffered Salt Solution (HBSS) to remove non-adhered cells. Adhered cells were fixed with 10% neutral buffered formalin (NBF) for 5 minutes, stained with 0.1% crystal violet for 5 minutes, rinsed twice with HBSS to remove any unabsorbed stain, and

air-dried. The number of adhered cells was determined using an optical density method previously described [Bernhardt, 1992 #1019], with slight modifications. Briefly, crystal violet was extracted from stained cells by adding 180  $\mu$ l of 70% ethanol per well, followed by rocking at RT for 2 hr. Optical density of the extracted crystal violet was read at 590 nm. Each cell line and each time point were performed in quadruplicate. Data are expressed as mean  $\pm$  s.e.m. For determination of percent cells adhered, a standard linear curve was generated by measuring the optical density of extracted crystal violet from known cell concentrations.

*Scrape Assay* – Log phase cells were placed in 60 mm tissue culture plates and grown to 100% confluency in complete medium supplemented with G418. The plates were rinsed in HBSS and a line of cells was removed from the center of the plates using a 1000  $\mu$ l Pipetman tip. Free floating cells, dislodged from the scrape line, were removed by rinsing with HBSS. Culture media free of serum and EGF was added and plates incubated for 24 hours at 37°C. To visualize motile cells within the scrape line, cells were fixed with 10% NBF for 5 minutes, stained with 0.1% crystal violet for 5 minutes, and excess stain removed with water. Cells were viewed on a Zeiss Axioscope 25 and representative scrape lines for each cell line photographed. All conditions were performed in triplicate and experiment performed in duplicate.

*Transwell Filter Motility Assay*- Transwell tissue culture filters with 8.0  $\mu$ m pore size (Falcon #3097) were pre-coated with 50  $\mu$ l of 10  $\mu$ g/ml porcine gelatin (Sigma) and gelatin solidified overnight at RT. Log phase cells were harvested with trypsin-EDTA and re-suspended in complete medium supplemented with only 0.1% horse serum. Fifty-thousand (50,000) cells per well were overlaid onto the top of the transwell filters (24 well format). Cells were stimulated to migrate across the filters by providing a chemoattractant (0.6% horse serum) in the assay chambers beneath the coated filter. After a 4 hour incubation at 37°C, cells were fixed in 10%

NBF for 5 minutes and stained with 0.1% crystal violet for 5 minutes. Non-motile cells on the top of the filter were removed by gentle scraping and cells that crossed through the filter pores were quantified photographically as previously reported [Bemis, 2000 #1008]. All conditions were performed in triplicate and experiment performed in duplicate. Data are expressed as mean  $\pm$  s.e.m.

*Invasion Assay*- Transwell filters were coated with 50  $\mu$ l of 200  $\mu$ g/ml porcine gelatin (Sigma) and allowed to solidify overnight to occlude the 8.0  $\mu$ m pores. Cells were suspended at 50,000 cells per well in 24-well filter plates (Falcon) using two different culture media, designed to evaluate growth factor dependency of invasion. The least restrictive media contained Ham's F12:DMEM (Gibco Life Technologies) supplemented with 0.1% horse serum, 10  $\mu$ g/ml insulin, 500 ng/ml hydrocortisone, 20 ng/ml EGF, 100 ng/ml cholera toxin, and 200  $\mu$ g/ml G418. The highly restrictive media consisted of Ham's F12:DMEM without any supplementation. Horse serum (0.6%) was utilized as the chemoattractant in the lower chamber. The number of invasive cells, evaluated 24 hours after plating, was quantified as for motility assay. All conditions were performed in triplicate and experiment performed in duplicate. Data are expressed as mean  $\pm$  s.e.m.

*3-Dimensional (3-D) Culture Model*- Log phase cells in complete medium plus G418 were overlaid as a single cell suspension onto a 100  $\mu$ l matrix substratum using 30,000 cells per well (96-well tissue culture plate; Nunclon). The matrix substratum consisted of a 1:1 mixture of Matrigel (Collaborative Biomedics) and complete medium plus G418. The development of organoids in this 3-D model is dependent on the migration of single cells into cell aggregates as previously described [Bemis, 2000 #1008]. Organoid development was monitored over 96 hours by inverted-light microscopy (Zeiss Axioscope 25) and photographed with a Polaroid camera at

100 X. After 72 hours, the organoids were treated with 0.01 mM of bromodeoxyuridine (BrdU) (Sigma) for 24 hours. Organoids were harvested at 96 h post-plating, stained with 0.1% trypan blue, fixed in methacarn for 10 minutes, paraffin embedded, and cut into 5  $\mu$ m sections.

*Immunohistochemical detection of BrdU*- Slides with 5  $\mu$ m sections were heat fixed for 20 minutes at 80°C. After clearing in xylene, tissue sections were rehydrated and endogenous peroxidase activity blocked with 3% peroxide. Slides were incubated in a 1:40 dilution of anti-BrdU (Beckton Dickinson) in PBS for 1 hour followed by incubation in a 1: 200 dilution of biotinylated rabbit anti-mouse secondary antibody (Dako) in PBS for 30 minutes. Biotin was detected by incubation in a 1:1000 dilution of conjugated HRP streptavidin (Gibco/BRL), followed by 10 minutes in 0.6 mg/ml of DAB (3,3'-diaminobenzidine tetrahydrochloride) in 20  $\mu$ l of 3% peroxide. Slides were counter-stained using a 1:10 dilution of Harris hematoxylin, rinsed with Scott's water, dehydrated in a series of ethanols, cleared in xylene, and then mounted with permount. The percentage of cells that incorporated BrdU was determined as previously described [Schedin, 2000 #1020]. Briefly, 20 randomly chosen fields were selected per cell line and photographed. The percent BrdU-positive cells that stained dark-brown, were counted from coded photographs independently by two investigators. Data are expressed as mean  $\pm$  s.e.m.

## Results

### *Characterization of the Stable Pooled Cell Lines*

In order to test the hypothesis that ESX imparts a transformed phenotype upon human mammary epithelial cells, we required a human mammary epithelial cell line that displays essentially a nontransformed phenotype and that does not express ESX. The MCF-12A cell line fulfills these criteria. MCF-12A cells are a mixed population of epithelial cells that grow as

patches of organized cuboidal cells surrounded by fibroblast-like cells in culture [Paine, 1992 #685]. They are EGF-dependent for proliferation, fail to grow in an anchorage-independent manner and fail to produce tumors in nude mice [Paine, 1992 #685][Wang, 1997 #1021]. To verify that MCF-12A cells failed to express ESX, MCF-12A cells were transiently co-transfected with a GFP-expressing plasmid and either control or HA-ESX vectors. The results show that control MCF-12A cells failed to express endogenous ESX, whereas exogenous HA-ESX was detected in MCF-12A cells transfected with pCGN2-HA-ESX (Fig. 1A), under conditions of equal GFP protein loading (Fig. 1B). Of note, endogenous ESX in MCF-12A cells was not detected by Western blotting, despite multiple attempts utilizing large amounts of nuclear protein (100  $\mu$ g) (data not shown).

Having verified that MCF-12A cells do not express ESX, these cells were stably transfected with pCGN2-HA-ESX, to evaluate the effects of ESX expression on mammary cell transformation. To control for the transfection and selection process, we used the vector-only control, pCGN2. As a positive control for transformation, we used pSV-Ras, which encodes the V12Ras oncogene and has been shown to confer the transformed phenotype in MCF-12A cells [Wang, 1997 #1021]. In addition, over-expression of the ETS family member, Ets-2, has been correlated with mammary tumorigenesis, but its precise role remains in question [Neznanov, 1999 #635]. Thus, we used pCGN2-HA-Ets-2, which encodes an HA-tagged version of Ets-2, to compare its effects with those of ESX and V12Ras. These pCGN2, pCGN2-HA-ESX, pCGN2-HA-Ets-2 or pSV-Ras plasmid DNAs were individually transfected into MCF-12A cells. Stable transfectants were selected and approximately 200 stably transfected clones were pooled to establish pooled cell lines denoted as pCGN2-P, ESX-P, Ets-2-P and V12 Ras-P. We chose to focus our study on pooled, stable transfectants, rather than clonal isolates, since the parental

MCF-12A population is morphologically heterogeneous and this heterogeneity appears to contribute to the normal, nontransformed phenotype [Kordon, 1998 #1005][Paine, 1992 #685].

To verify the expression of exogenous HA-ESX in the stable ESX-P cells, we performed RT-PCR analysis using oligonucleotide primers specific for the HA-tagged ESX cDNA. Figure 2, lanes 1 and 2 show that nontransfected parental MCF-12A cells nor vector control pCGN2-P cells, respectively, expressed detectable levels of HA-ESX mRNA. By contrast, HA-ESX mRNA was readily detected in ESX-P cells (Fig. 2, lane 3). DNA sequencing of the upper, dominant band verified that the product was indeed authentic HA-ESX (data not shown). Also, Fig. 2, lanes 6 and 7, reveal that Ets-2-P and V12Ras-P cell lines failed to express HA-ESX mRNA. In addition, we verified that exogenous HA-Ets-2 was expressed in the Ets-2-P cells using a similar RT-PCR strategy (data not shown).

While we have clearly documented HA-ESX mRNA expression in the ESX-p cells, we have been unable to detect HA-ESX protein, despite repeated attempts using either Western blot analysis of whole cell or nuclear extracts, or a two-step procedure involving immunoprecipitation followed by Western blot analysis. These results indicate that HA-ESX protein is expressed at a low level that appears to be below current detection methods. Indeed, using GFP as a surrogate marker for ESX and confocal microscopy to amplify the signal, we have been able to detect GFP-ESX fusion protein expression in stably transfected MCF-12A cells (J. D. Prescott & A. Gutierrez-Hartmann, unpublished data).

#### *ESX, Ets-2 and V12Ras Confer EGF-Independent Growth*

The parental MCF-12A cells have been reported to be highly dependent on exogenous EGF for cell growth [Paine, 1992 #685]. One characteristic of cellular transformation is loss of

growth factor dependence [Hanahan, 2000 #1022]. In order to evaluate the EGF dependence of pCGN2-P, ESX-P, Ets-2-P and V12Ras-P cells for growth, we determined the growth rates of each of these cell populations in media containing reduced serum (1% horse serum) in the presence or absence of EGF (20 ng/ml). As shown in Figure 3A, the parental nontransfected MCF-12A and the pCGN2-P cells had a limited ability to grow in media that lacked EGF, whereas ESX-P, Ets-2-P and V12-Ras-P cells grew more robustly than the parental or pCGN2-P controls. Indeed, by the fifth day, the number of cells in control cultures was declining, while the cell number in ESX-P, Ets-2-P and V12-Ras-P cultures continued to increase. The growth advantage that the ESX-P, Ets-2-P and V12-Ras-P cells displayed in restrictive media were indistinguishable from each other (Fig. 3A). The differences in cell growth between control and experimental lines is unlikely to be attributed to differential plating efficiency, since the number of adhered cells 24 hours after initial plating of these various cell lines was statistically indistinguishable from each other (Fig. 3A, 1 day). In addition, while ESX-P, Ets-2-P and V12-Ras-P cells grew better than controls in the restrictive media, they grew similarly to controls when plated in complete media (Fig. 3B). Thus, the presence of ESX, Ets-2 or V12-Ras did not confer a significant growth advantage, when cells were plated in EGF-containing media. Finally, the growth rate of all the cell lines was significantly higher in EGF-containing media compared to restrictive media, demonstrating that ESX-P, Ets-2-P and V12-Ras-P cells retain their ability to respond to added EGF.

#### *Phosphorylated Levels of MAP Kinase in Stable Populations*

Having shown that ESX-P, Ets-2-P and V12-Ras-P cells were able to proliferate in the absence of added EGF (Fig. 3A), we hypothesized that an autocrine loop had been established in

MCF-12A cells by the expression of ESX, Ets-2 and V12-Ras. If this was the case, then downstream signaling molecules, such as MAP kinase, should be activated in the absence of EGF and serum. To determine the levels of phosphorylated MAP kinase in pCGN2-P, ESX-P, Ets-2-P and V12-Ras-P cells, these lines were grown in serum-depleted (0.1%) media lacking EGF. Under these growth conditions, the pCGN2-P cells displayed little to no detectable levels of phosphorylated MAP kinase (Fig. 4). In contrast, in these serum-starved and growth factor-depleted conditions, the ESX-P, Ets-2-P and V12-Ras-P cells displayed readily detectable levels of phosphorylated MAP kinase. The data in Fig. 3A was quantitated by densitometry and normalized to the actin levels, and revealed that phospho-MAPK levels were equivalent for the ESX-P and Ets-2-P cells and that these levels were approximately 20-fold greater than that of vector control cells (Fig. 4, upper). Of note, the V12-Ras-P cells displayed a 200-fold increase in phospho-MAPK levels compared to controls cells (Fig. 4, lower). These data are consistent with the proliferation results (Fig.3A), and suggest that ESX, Ets-2 and V12-Ras have each established an autocrine loop, resulting in constitutive phosphorylation of MAPK and a growth advantage to cells under growth-restrictive conditions.

#### *Anchorage-independent Growth of ESX-P, Ets-2-P and V12-Ras-P Cells in Soft Agar*

The transfection of constitutively active Ras into WT MCF-12A cells with has been shown to give these cells the ability to grow in soft agar [Wang, 1997 #1021]. Such anchorage-independent growth is an accepted indicator of transformation [Hanahan, 2000 #1022]. In order to assess the transformation potential of HA-ESX and HA-Ets-2 in MCF-12A cells, the ability of stable pooled populations of cells to form colonies in the restrictive soft agar assay was determined. At four weeks, vector control plates had very few detectable colonies (Fig. 5,

pCGN2-P). HA-ESX transfectants had numerous small (0.1 mm) to medium (0.6 mm) foci (Fig. 5, ESX-P). HA-Ets-2 and V12-Ras stable cells had fewer, but larger foci ranging from 0.5 to 2 mm, which were easily detectable with the naked eye (Fig. 5, Ets-2-P and V12Ras-P).

#### *ESX, Ets-2 and V12Ras Confer a Functional Mesenchymal Phenotype in MCF-12A Cells*

A hallmark characteristic of highly metastatic epithelial tumor cells is the acquisition of a mesenchymal phenotype [Hay, 1995 #1016]. In order to determine whether ESX, Ets-2 or V12-Ras are able to induce an epithelial to mesenchymal transition in MCF-12A cells, we measured cellular properties associated with the mesenchymal phenotype, including adhesion, motility and invasiveness. Figure 6 shows the ability of pCGN-P, ESX-P, Ets-2-P and V12-Ras-P cells to adhere to a plastic substratum. Seventy-five minutes after initial plating, ~25% of pCGN-2-P control cells were adhered, while ~70% of the ESX-P and Ets-2-P cells were adhered. The V12-Ras-P cells adhered more rapidly (50% at the earliest time point of 30 min) and more completely (essentially 100% by 45 min). At 24 hours after plating, the plating efficiency was equivalent for all cell lines (data not shown), an observation consistent with data presented in Fig. 3.

Having established increased adhesiveness of the ESX-P, Ets-2-P and V12-Ras-P cells, we next evaluated whether these cells also display increased motility using scrape-wounding and transwell filter assays. In the scrape motility assay, confluent cultures were wounded by scraping cells to expose a linear cell-free zone. The cell motility that is measured in the scrape assay relies on the ability of cells to overcome cell-cell and cell-matrix interactions. In the culture conditions used here, we minimized the contribution of cell proliferation to the re-population of the scrape zone, by utilizing serum-free and growth factor-depleted media. The ability of cells to re-populate this zone was measured 24 hours after wounding (Fig. 7). In serum-free culture

conditions, pCGN2-P cells failed to re-populate this zone (Fig. 7, upper left), while ESX-P and Ets-2-P cells re-populated approximately 50% of the scraped zone (Fig. 7 upper right and 7 lower left). The V12-Ras-P cells displayed the highest motility and were able to re-populate the entire zone within 72 hr (Fig. 7 lower right).

Visual inspection of the scrape zone revealed notable differences in cell morphology between the cell lines. pCGN2-P cells produced two distinct morphological phenotypes, a densely packed, darkly stained cuboidal-like epithelial cell that formed distinct islands (Fig. 7, upper left, dark arrows) and more loosely packed, lightly stained elongated cells that surrounded these islands (fine arrow). These two distinct cell phenotypes have been previously described for MCF-12A cells [Paine, 1992 #685]. Remarkably, in the ESX-P, Ets-2-P and V12-Ras-P cells there is a selective loss of the cuboidal islands, while the fibroblast-like cells were maintained (Fig. 7). Of note, the V12-Ras-P cells acquired additional morphological features, manifested by a higher degree of homogeneity and a particularly elongated cell shape.

To gain further insights of the motile properties gained by ESX expression, we also tested MCF-12A cell motility using the short-term (4 hr) trans-well assay, wherein the ability of single cells to migrate independent of cell interactions and in response to a chemo-attractant is measured. As shown in Fig. 8, the pCGN2-P vector control cells displayed very low motility (~12 cells/field; set to 1), while the ESX-P cells revealed approximately 6.5-fold increased motility (~80 cell/field). The Ets-2-P cells also demonstrated an increased motility compared to control pCGN2-P cells, but an apparent reduced motility compared to ESX-P cells. The V12-Ras-P cells revealed the highest motility (~150 cells/field; 11.5-fold). While Fig. 8 depicts a representative experiment performed in triplicate, the same trends in motility observed for the ESX-P, Ets-2-P and V12-Ras-P cells were reproducibly obtained in three separate experiments.

Thus, using two different experimental approaches to measure cell motility, we detected an increased motility in the ESX-P, Ets-2-P and V12-Ras-P cells in comparison to control pCGN2-P cells. Although motility was similarly increased in these three cell lines (ESX-P, Ets-2-P and V12-Ras-P cells), an analysis of cell morphology in the trans-well assay revealed that the ESX-P and ETS-2-P cells had very different cell shape compared to the V12-Ras-P cells. Figure 9 shows representative fields of the bottom of trans-well filters, stained with crystal violet. The upper left panel shows that very few pCGN2-P cells migrated through the filter. The arrow points to a filter pore, and a single stained motile cell is noted just above and to the left of the arrow. The ESX-P panel shows numerous migratory cells, and these cells acquired a flattened morphology with increased surface area and prominent broad lamellapodia (arrow). Panel Ets-2-P depicts cells with both large ruffled lamellopodia (arrow) and occasional thin filopodia. In contrast, the morphology of the V12Ras-P cells was highly elongated and fibroblast-like, with two to three prominent filopodium per cell (arrow). The presence of lamellopodium in the ESX-P and Ets-2-P cells, and filopodium in V12-Ras-P cells, correlates with the motile phenotype, since these cellular structures are found at the leading edge of actively migrating cells [Lauffenburger, 1996 #1012].

Having established that the ESX, Ets-2 and V12-Ras genes conferred a motile phenotype to MCF-12A cells, and since increased motility is required for invasiveness, we next sought to determine whether these various stable cell lines displayed enhanced invasive properties. The method used to test for invasion was the trans-well filter 24 hour invasion assay. In this assay, cells are over-layed onto filters in which the 8  $\mu$ m pores are occluded with gelatin so that the transit of cells to the lower chamber requires both active matrix degradation and motility. Figure 10 shows the invasion results of the four stable cell lines in serum-free and EGF-free culture

medium, either in the presence (moderately restrictive media) or absence (highly restrictive media) of insulin, hydrocortisone and cholera toxin. Independent of media conditions, control pCGN2-P cells displayed low invasion (~40-50 cells/field), while the ESX-P, Ets-2-P and V12Ras-P displayed marked invasion that ranged from 3-6-fold over controls (Fig. 10). Of note, the ability of the ESX-P, Ets-2-P and V12Ras-P cells to invade in the absence of any added growth factors or serum demonstrates that this phenotype is totally independent of exogenous growth factors. These results are in agreement with our previous data showing that the ESX-P, Ets-2-P and V12Ras-P cells are able to proliferate and activate MAPK in growth factor-depleted conditions and are consistent with the idea that an autocrine loop has been established by the expression of ESX, Ets-2 or V12Ras that contributes to cell proliferation, motility and invasion.

#### *MCF-12A Cells Recapitulate Normal Mammary Development in a 3D Culture Assay*

We sought to expand the utility of the MCF-12A cell system by establishing an in vitro, three-dimensional (3D) culture assay designed to mimic normal mammary development in vitro. Our rationale for this approach was that 3D assays have been demonstrated to rapidly distinguish between transformed and nontransformed mammary epithelial cells in culture [Weaver, 1996 #1007]. For our studies, we sought to determine the effects of ETS transcription factors and oncogenic V12Ras on the ability of MCF-12A cells to develop into mammary duct-like structures. In order to address this question, we first needed to establish whether MCF-12A cells were capable of recapitulating normal mammary gland-like structures in 3D culture. Single cell suspensions of MCF-12A cells were overlayed onto reconstituted basement membrane substratum (Matrigel) and organoid development analyzed, as previously described [Bemis, 2000 #1008]. In this assay, the MCF-12A cells displayed a time-dependent organization into discrete

mammary-like structures. Within the first 24 hours, MCF-12A cells were observed to structure into solid 3-dimensional organoids (data not shown). Between 24 and 72 hours, MCF-12A organoids hollowed into both alveolar- and duct-like structures with central lumens, as shown in Fig. 11, left three panels. An alveolar-like structure is depicted in the upper left panel with the asterisks denoting cavitation and the arrow pointing to an apoptotic cell. Although the precise mechanism for lumen formation is unknown, cytological data suggest that internal cells die by apoptosis (Fig. 11). In the 3-D model, internal cells undergo apoptosis presumably because normal, non-transformed epithelial cells are substratum dependent for viability [Humphreys, 1996 #1024; Coucouvanis, 1995 #1023]. In comparison to parental MCF12A cells, the pCGN2-P cells organized only into duct-like structures (Fig. 11, right three panels). In addition, fewer of these pCGN2-P organoids hollowed (Fig. 11, upper right panel). However, both the parental MCF-12A and pCGN2-P cells maintained several features of normal mammary-like epithelium, including morphological evidence of apical-basal polarity, cell-cell adhesions, organoid size (ie, organoids that appropriate in vivo duct and alveolar size) and lack of invasiveness into surrounding matrix.

#### *ESX-P, Ets-2-P and V12Ras-P Cells Form Aggressive Tumor-Like Structures in 3D Culture*

Having established that MCF-12A and control pCGN2-P cells were capable of forming normal mammary gland-like structures in a 3D cultures, we next determined the ability of ESX-P, Ets-2-P and V12Ras-P cell lines to organize in 3D culture. All three of these cell lines failed to organize into duct-like structures. Instead, these cell lines formed disorganized solid structures consistent with an aggressive, tumor-like phenotype (Fig. 12). Within the first 24 hours, the ESX-P, Ets-2-P and V12Ras-P cell lines formed large, solid organoids that lacked cell polarity

and failed to hollow, because unlike parental MCF-12A cells, internal cells failed to die (Fig.12, top and left three panels). Failure of internal cells to undergo apoptosis is further evidence that ESX-P, Ets-2-P and V12Ras-P cells are anchorage-independent for cell viability. Moreover, many of the tumor-like organoids formed by these cell lines were much larger than those formed by the parental and pCGN-2P cells (compare top panel of Fig. 12 to Fig. 11). This result indicates that these tumor-like organoids failed to appropriately limit the number of cells contributing to each organoid, an attribute previously identified in tumorigenic mammary epithelial cells in 3D culture [Weaver, 1996 #1007]. By 72 hours, the ESX-P, Ets-2-P and V12Ras-P organoids exhibited features not seen in control organoids. Specifically, cells from the ESX-P, Ets-2-P and V12Ras-P organoids had locally invaded their surrounding matrix (Fig. 12, right three panels, arrowheads). In addition to acquisition of motility and invasiveness, these invasive cells displayed further evidence of EMT, as shown by their loss of cell-cell adhesion and fibroblast-like shape with prominent invasive filopodia (Fig. 12, arrowheads). Taken together, these data reveal a step-wise progression in tumor-like organoid development, manifested by the initial formation of large, solid 3D structures, where internal cells failed to die, followed by the formation of a peripheral zone of migrating cells that have acquired the EMT phenotype.

*ESX-P, Ets-2-P and V12Ras-P Cells Have Reduced Proliferation Rates in 3D Culture:*

As shown in Fig. 3, we have demonstrated that the ESX-P, Ets-2-P and V12Ras-P cells have a growth advantage in EGF-depleted media. Because the 3D culture conditions more closely mimic the in vivo cell-cell and cell-substratum architecture, we sought to determine the effects of ESX, Ets-2 and V12Ras gene expression on the proliferation rates of these cells in the

3D-culture model. Contrary to our expectations, the ESX-P, Ets-2-P and V12Ras-P cells displayed proliferation rates that were ~5- to 6-fold lower compared to that of the pCGN-2-P control cells (Fig. 13). Specifically, in a 24 hour period, 32% of the pCGN-2-P cells displayed proliferation, as measured by immuno-histochemical quantitation of BrDU incorporation (Fig.13). Whereas the ESX-P, Ets-2-P and V12Ras-P cells displayed much lower levels of proliferation that measured 5%, 8% and 13%, respectively. Morphological analysis of 5  $\mu$ m sections of organoids revealed distinct patterns of BrDU incorporation in the control pCGN-2-P cells compared to the ESX-P, Ets-2-P and V12Ras-P cells (Fig. 14). In the pCGN-2-P cells, BrDU incorporation was preferentially localized to those cells at the periphery of the organoid (Fig. 14, upper left panel, arrow), indicating that proliferation occurred in cells contacting the matrix substratum. By contrast, BrDU incorporation in the ESX-P (upper right panel), Ets-2-P (lower left panel) and V12Ras-P (lower right panel) cells was scattered and random throughout the solid tumor-like lesion (large arrows). Of interest, ESX-P, Ets-2-P and V12Ras-p cells that displayed the EMT phenotype and that had migrated away from the central solid tumor, were not observed to incorporate BrDU (Fig.14, arrowheads).

## Discussion

This paper provides several key contributions that further our understanding of transformation of mammary epithelial cells by Ets factors. Importantly, this is the first demonstration of the ability of transfected Ets DNA to act as a transforming gene in mammary epithelial cells in vitro. Here, we show that the Ets factors ESX and Ets-2 are each capable of conferring aggressive, metastatic properties to immortalized, but otherwise normal human mammary epithelial MCF-12A cells. Specifically, ESX and Ets-2 stably-transfected MCF-12A cells acquired growth factor- and anchorage-independent growth, and displayed enhanced motility and invasiveness in 2D culture. Moreover, in 3D organoid assays, it was evident that ESX and Ets-2 induced a functional epithelial-to-mesenchymal transition, similar to that induced by oncogenic V12Ras. Interestingly, while we identified a proliferative advantage to the ESX-P, Ets-2-P and V12Ras-P cells in 2D culture in growth restrictive conditions, these same cells had significantly reduced proliferative capacity in 3D culture. This observation suggests that the cell microenvironment regulates a switch between mitosis and cell motility in transformed MCF-12A cells, an observation that may have potential clinical significance. Specifically, in vivo, metastatic breast cancer cells reside in a milieu similar to the 3D culture conditions, and thus may be relatively hypoproliferative and resistant to chemotherapeutic agents targeting rapidly dividing cells.

Ets factors, particularly Ets-2 and Pea-3, have been implicated in mammary tumorigenesis [Shepherd, 2000 #826; Baert, 1997 #44; Benz, 1997 #63; Gilles, 1997 #295; Watabe, 1998 #949; Dittmer, 1998 #204]. The most definitive reports to date demonstrate that loss of Ets factor function suppresses both mammary tumor cell transformation and tumor formation. Expression of a dominant-negative Ets construct in several mammary epithelial tumor cell lines resulted in reversion of anchorage-independent cell growth and cellular invasiveness in

vitro [Sapi, 1998 #783; Delannoy-Courdent, 1998 #192]. In addition, bi-transgenic *ets-2* knock out/MMTV-PyMT mice displayed reduced mammary tumor progression [Neznanov, 1999 #635] and bi-transgenic *pea3* knock out/ MMTV-*neu* mice revealed delayed mammary tumor onset and reduced multiplicity [Shepherd, 2001 #1025]. ESX is an ETS transcription factor family member that may be particularly relevant in breast cancer due to its epithelial-specific mode of expression. ESX maps to human chromosome 1q32.1 in a region that is amplified in up to 50% of early-stage breast cancers and in DCIS. In addition, ESX RNA is over-expressed in human breast cancer [Tymms, 1997 #912; Chang, 1997 #135]. Similarly, we have identified increased ESX expression in chemically-induced rat mammary tumors (data not shown). As an initial attempt to determine the effects of ESX on mammary cell transformation, we previously reported that ESX-nonexpressing MCF-12A cells, transiently transfected with an ESX expression vector, form significantly more colonies than control transfected cells [Eckel, 2001 #1006]. Conversely, we also addressed the effects of ESX loss-of-function in ESX-expressing T47D mammary tumor cells. Transient transfection of either an anti-sense or dominant-negative ESX construct into ESX-positive T47D cells resulted in considerable reduction in colony formation of these cells [Eckel, 2001 #1006]. The data presented here corroborate and extend our previous findings and show that ESX expression is sufficient to transform immortalized mammary epithelial cells to a highly aggressive, transformed phenotype.

Oncogenic cell transformation is correlated with growth factor-independent proliferation and this proliferation is frequently associated with establishment of autocrine loops that constitutively activate the MAPK pathway. For example, oncogenic Ras has been shown to establish EGF-related autocrine loop pathways by inducing TGF- $\alpha$ , amphiregulin and HB-EGF [Falco, JCI, 85:1990; Gangarosa, JBC, 272:1997]. Here we show that the ability of ESX

and Ets-2 to confer EGF-independent proliferation to MCF-12A cells correlates with constitutive activation of MAPK (Fig. 4). This observation suggests that the downstream targets of ESX and Ets-2 include genes for growth factor ligand(s) and/or their receptor(s). Importantly, while ESX and Ets-2 were able to impart a growth advantage to MCF-12A cells cultured in the absence of EGF, all of the stable cell lines (ESX, Ets-2 or V12Ras) displayed increased proliferation rates when treated with exogenous EGF (Fig.3 A vs B). This observation reveals that ESX, Ets-2 and V12-Ras are unable to confer the full mitogenic effects of exogenous EGF. For example, the total number of cells was 5-fold lower in the ESX, Ets-2 or V12Ras stables in the absence of EGF (~40,000) compared to the same cells in the presence of EGF (~200,000). One interpretation of these data is that EGF activates pleiotropic proliferative pathways in MCF12-A cells, whereas ESX, Ets-2 or V12Ras may be activating a more restrictive proliferative response. Alternatively, EGF may activate the MAPK pathway transiently, resulting in a robust proliferative signal; whereas ESX, Ets-2 and V12-Ras activate MAPK persistently, which subsequently dampens the proliferative response. This type of differential proliferative response to transient vs persistent MAPK activation has been previously reported (Traverse, Seedorf et al. 1994). Nevertheless, the ETS-factor mediated proliferative response provides the ESX-P and Ets-2-P mammary epithelial cells a distinct growth advantage, consistent with the demonstrated mammary tumor suppression observed with haplo-insufficiency for *ets-2* and *pea-3* in MMTV-PyMT and MMTV-*neu* mice, respectively [Neznanov, 1999 #635] [Shepherd, 2001 #1025].

While growth factor-independent proliferation is a key event in early stages of cellular transformation, a hallmark of overt metastasis is conversion of a tumor cell from an epithelial to a mesenchymal phenotype. During embryonic development, conversions between epithelium and mesenchyme occur regularly to allow for morphogenesis (Cunha 1994; Hay 1995). However, in

normal adult tissue, EMT occurs only in epithelial cells during pathological wound healing and metastasis (Hay 1995). Three interrelated events need to occur for an epithelial cell to undergo an EMT and become metastatic: 1) changes in cell adhesion, 2) reorganization of the actin cytoskeleton to generate contractile force required for motility, and 3) production of active matrix degrading enzymes to penetrate ECM barriers. Here, we have determined that ESX, Ets-2 and V12Ras induce functional attributes of each of these EMT phenotypes in MCF-12A cells.

In this study, each EMT phenotype was identified by multiple methodological approaches. The property of altered adhesion was directly detected by increased adhesion in the 90 min adhesion assay, and indirectly inferred by the ability of ESX-P, Ets-2-P and V12Ras-P cells to grow in soft agar independent of cell-cell contacts. Additionally, we observed formation of solid tumor-like organoids in the 3D assay. Solid organoid development is significant because non-transformed mammary epithelial cells undergo cell death when contacts with basement membrane proteins are lost (Li, Aggeler et al. 1987; Blum, Ziegler et al. 1989; Boudreau, Simpson et al. 1995), resulting in the formation of hollow duct-like structures. The requirement for substratum contact for epithelial cell viability is considered to be the mechanism by which solid cords of epithelial cells cavitate during normal duct development in vivo [Humphreys, 1996 #1024; Coucouvanis, 1995 #1023], and is likely to account for the cavitation observed in nontransformed MCF12A organoids in this study. By contrast, the ability of ESX-P, Ets-2-P and V12Ras-P cells to form solid 3D structures demonstrates loss of this cell adhesion requirement and implicates changes in membrane adhesion molecules. Integrins are the primary adhesion molecules by which cells interact with the ECM, while E-cadherin is the primary adhesion molecule by which cells interact with neighboring cells [Angst, 2001 #1010; Danen, 2001 #1009]. Previously published reports have shown that ETS factors regulate key adhesion

molecules such that cell-cell contacts mediated by cadherins are diminished and cell-ECM contacts mediated by integrins are altered. [Gilles, 1997 #295; Oda, 1999 #665; Rodrigo, 1999 #759; Takaoka, 1998 #873]. Our functional assays demonstrating altered adhesion support these earlier studies and indicate that ESX-P and Ets-2-P cells bypass homeostatic contact mechanisms mediated by cell adhesion, resulting in cells with a distinct survival advantage under conditions of altered cell-ECM interactions.

The observed changes in adhesive properties in the ESX-P, Ets-2-P and V12-Ras-P cells are predictive of increased motility. Indeed, increased motility in the ESX-P, Ets-2-P and V12-Ras-P cells was detected by three independent assays: scrape-injury, transwell filter migration and 3D organoid development. Upon induction of motility, actin is distributed into contractile actin-myosin filaments called stress fibers, which anchor to the ECM via integrins at the cell's leading edge (Hall 1998). Motile cells display two prominent membrane protrusions at the leading edge, large, broad lamellipodium or slender filopodium, [Lauffenburger, 1996 #1012; Stossel, 1999 #1011]. Consistent with the motile phenotype, the ESX-P, Ets-2-P cells, but not control cells, showed formation of broad lamellipodia (Fig. 9). In contrast, the motile V12-Ras-P cells showed primarily filopodia formation (Fig. 9). These distinct motile phenotypes suggest that Ets factors activate a different motility pathway than V12Ras. Candidate regulators of lamellipodium and filopodium are members of the Rho family of small GTPases; Rho, Rac and Cdc42 (Bar-Sagi and Hall 2000). Specifically, activation of Rac induces lamellipodium, implicating Rac as a downstream effector of both ESX and Ets-2 Ets transcription factors in MCF12A cells. In support of our observations that gain of Ets function induces motility, expression of dominant-negative Ets-1 in murine MMT mammary tumor cell line resulted in inhibition of cell motility and enhancement of cell adhesion as measured by loss of cell

scattering [Delannoy-Courdent, 1998 #192]. Similarly, expression of a dominant-negative Ets-2 in human BT20 breast cancer cell line resulted in a loss of motility [Sapi, 1998 #783].

In order for breast tumor cells to invade local tissue and gain access to the lymphatics and circulatory systems, they must be able to clear a path through extracellular matrix barriers [Benaud, 1998 #1014; Basset, 1993 #1013][Duffy, 1999 #1015]. Evidence for acquisition of an invasive phenotype in ESX-P, Ets-2-P and V12-Ras-P cells was generated using two distinct assays. In the transwell filter invasion assay, filter pores were occluded with gelatin so that secretion of gelatinase by ESX-P, Ets-2-P and V12-Ras-P cells was required for invasiveness (Fig. 10). In the 3D organoid assay, invasiveness of ESX-P, Ets-2-P and V12-Ras-P cells was measured by the ability of cells to disseminate from the primary organoids and invade into surrounding reconstituted basement membrane (Fig. 12). Of relevance to our observation that ESX and Ets-2 increase invasiveness of MCF12A cells, the Ets proteins Ets-1, ER81, PEA3, and E1AF have been shown to regulate a repertoire of genes that govern invasiveness in epithelial and mesenchymal cells, including collagenase, urokinase, matrylsin, and MT1-MMP (Shepherd and Hassell 2000).

Finally, we provide evidence that in a physiologically-relevant environment (3D culture on reconstituted basement membrane), transformed cells significantly down-regulate mitosis in comparison to nontransformed cells. In addition, cells that had undergone an EMT were not observed to synthesize DNA, implying that a switch between mitogenesis and motogenesis occurs in 3D culture. Suppression of mitosis in epithelial cells that have undergone an EMT has been previously reported. Rat bladder carcinoma NBT-II cells transition to a mesenchymal phenotype when treated with acidic fibroblast growth factor ( $\alpha$ FGF) (Savagner, Boyer et al. 1994). When NBT-II cells are simultaneously treated with  $\alpha$ FGF and growth media, these cells

failed to incorporate 3H-thymidine. Furthermore, in the scrape-wounding assay, NBT-II cells located at the edge of the wound underwent EMT and did not synthesize DNA, whereas confluent cells within the monolayer synthesized DNA. More recently, it has been demonstrated that FGF can stimulate cell movement in all phases of the cell cycle except G2 and M, further supporting a role for a molecular switch between mitosis and motility (Bonneton, Sibarita et al. 1999). How the local microenvironment (2D vs 3D) discriminates between growth and motility is an area of active research, and is likely due to a myriad of signaling interactions between adhesion molecules, growth factors, and the actin cytoskeleton, all of which can be dynamically regulated by the microenvironment. Our observation that ESX-P, Ets-2-P and V12Ras-P cells are preferentially motogenic in 3D culture may have clinical impact. Specifically, tumorigenic cells that have undergone an EMT may be particularly resistant to standard chemotherapeutic drugs that target actively dividing cells.

## FIGURE LEGENDS

**Fig 1. Expression of ESX in MCF-12A cells.** MCF-12A human breast cells were co-transfected by electroporation with the plasmids encoding enhanced green fluorescent protein (pEGFP) and either the HA-ESX expression plasmid (pCGN-2 HA-ESX) or the empty vector (pCGN2), as described in Materials and Methods. Transfected cells were isolated by FACS based on EGFP fluorescence, lysed in hypotonic lysis buffer, and equal protein amounts were loaded onto a 10% SDS-PAGE gel, followed by Western blotting. The blot was probed sequentially with antibodies directed against ESX (upper panel) and EGFP (lower panel).

**Fig 2. RT-PCR analysis of HA-ESX expression in MCF-12A stable pools.** Reverse transcriptase-polymerase chain reaction (RT-PCR) was performed on RNA isolated from various pooled populations of stable MCF-12A, as described in Materials and Methods. Twenty-five cycles of PCR were carried out using oligonucleotide primers specific for HA-ESX. The PCR products were loaded onto a 1% agarose gel, electrophoresed and stained with ethidium bromide. Lane 1: Wild-type MCF-12A cells. Lane 2: Vector alone stable cells. Lane 3: HA-ESX stable cells. Lane 4: HA-Ets-2 stable cells. Lane 5: V12-Ras stable cell lines.

**Fig 3. ESX-P, Ets-2-P and V12Ras-P cells demonstrate enhanced EGF-independent proliferation.** Proliferation rates of wild-type and pCGN2-P, ESX-P, Ets-2-P and V12Ras-P stable cell lines were determined in media containing reduced serum (1% horse serum) in the absence of EGF (upper panel), or in the presence of 20 ng/ml EGF (lower panel). Cells were plated at an initial density of 10,000 cells per plate. At 24-hr intervals, cells were harvested from

plates and manually counted in triplicate using a hemacytometer, for a total of five days. Data represent mean cell counts  $\pm$  SEM.

**Fig 4. ESX-P, Ets-2-P and V12Ras-P stable cell lines exhibit elevated levels of activated p44/42 MAP kinase in the absence of EGF.** Wild-type and pCGN2-P, ESX-P, Ets-2-P and V12Ras-P stable cell lines were serum-starved for 12 hours in media containing 0.1% horse serum and lacking EGF. Cell lysates were prepared from wild type MCF-12A cells (lane 1), vector-only stable cells (lane 2) and stable cell lines expressing either HA-ESX (lane 3), HA-Ets-2 (lane 4) or V12-Ras (lane 5). Equal amounts of total cellular protein were electrophoresed on 10% PAGE and analysed by Western blot. Upper panel depicts a representative Western blot probed with an antibody specific for phosphorylated p44/42 MAPK (pMAPK). Lower panel depicts the same Western blot stripped and re-probed with an antibody against  $\beta$ -actin (Actin), to control for loading differences between samples.

**Fig 5. Colony formation assay of stable pCGN2-P, ESX-P, Ets-2-P and V12Ras-P cells in soft agar.** Twenty thousand cells from each line were plated in soft agar. Representative photographs taken at four weeks show colonies or the lack thereof for pCGN2 control vector (upper left), HA-ESX (upper right), HA-Ets-2 (lower left) and V12Ras (lower right) transfected stable cell lines. Size bar equals 2 mm.

**Fig 6. Cell adhesion is altered in ESX-P, Ets-2-P and V12Ras-P cells.** Ability of cells to adhere to plastic substratum was measured over a 75 min time course. Adherent cells were stained with 0.1% crystal violet and dye extracted with ethanol. Adherent cell number was

quantified by determining optical absorbance at 590 nm. Bars represent % adherent cells at indicated time points after initial plating. Experimental conditions were performed in triplicate and data are expressed as mean  $\pm$  SEM. ESX-P, Ets-2-P and V12Ras-P cells revealed significantly increased adherence at 75 min post-plating compared to vector control cells,  $p < 0.008$ ,  $0.001$  and  $0.006$ , respectively, (2-tailed t-test).

**Fig 7. Cell motility was increased in ESX-P, Ets-2-P and V12Ras-P cells in the scrape assay.**

Cells in 2-D culture were wounded by scraping confluent monolayers. The ability of the cells to re-populate the scrape zone in the presence of media devoid of serum and growth factors was determined after 24 hr. pCGN2-P (upper left panel), ESX-P cells (upper right panel), Ets-2P cells (lower left panel) and V12Ras-P cells (lower right panel). The pCGN2-P cell monolayer consisted of two distinct cell populations (upper left), fine arrow depicts elongated fibroblast-like cells and wide arrows depict dense, epithelial like colonies. Experimental conditions performed in triplicate, experiment in duplicate. Representative data shown. Size bar equals 100  $\mu$ m.

**Fig 8. Migration of cells through Boyden chamber filters was increased in ESX-P, Ets-2-P and V12Ras-P cells.** Filters with 8  $\mu$ m pores were coated with 10  $\mu$ g/ml gelatin. Cells were plated in upper wells of chambers using 0.5% FBS as a chemo-attractant in lower wells. Cell motility was measured as a function of the number of cells that traversed from the upper chamber to lower chamber within 4 hr. Data are expressed as mean  $\pm$  SEM. ESX-P, Ets-2-P, and V12Ras-P cells displayed significantly higher motility than pCGN2-P control cells,  $p < 0.0001$  for all three cell lines (two-tailed t test). Experimental conditions performed in triplicate, experiment in duplicate.

**Fig 9. Motile ESX-P and Ets-2-P cells predominantly display lamellopodia, while V12Ras cells display filopodia.** Cells that traversed the 8  $\mu$ m filter in the transwell filter motility assay were stained with 0.1% crystal violet and representative areas photographed. Upper left panel shows a single migratory CGN2-P cell and numerous empty 8  $\mu$ m filter pores (pore denoted by arrow). Actively motile ESX-P cells (upper right panel) displayed prominent lamellopodia (arrow). Motile Ets-2-P cells (lower left panel), displayed both ruffled lamellopodia (arrow) and filopodia, while motile V12Ras-P cells (lower right panel) displayed prominent filopodia (arrow). Size bar equals 50  $\mu$ m.

**Fig 10. Invasion through modified Boyden chamber filters is increased in ESX-P, Ets-2-P and V12Ras-P cells.** Eight  $\mu$ m filter pores were occluded with 200  $\mu$ g/ml gelatin. Cells were plated in upper wells of chambers using 0.5% FBS as a chemo-attractant in lower wells. Cell transit from upper chamber to lower chamber requires degradation of gelatin within pores. Cell invasion was measured as the number of cells that traversed through filter pores within 24 hr. Data are expressed as mean  $\pm$  SEM. ESX-P, Ets-2-P, and V12Ras-P cells displayed significantly higher invasiveness than pCGN2-P control cells,  $p < 0.0001$  for all three cell lines (two-tailed t test). Experimental conditions performed in triplicate, experiment in duplicate.

**Fig 11. MCF 12A and pCGN-2-P cells recapitulate aspects of mammary gland development in 3D culture.** MCF12A and vector control pCGN2-P cells were overlaid onto thick, reconstituted EHS basement membrane as single cell suspensions. Single cell aggregation into organoids was monitored for 72 hr and organoids processed for 5  $\mu$ m histological sections and

stained with hematoxylin and eosin. Left three panels depict typical organoid morphologies observed with MCF 12A cells. Upper left panel shows an alveolar-like structure with hollowed lumen (asterisks) and evidence of an internal apoptotic cell (arrow), 400X. Middle left panel shows hollowed duct-like organoid, 400X, and lower left panel shows high magnification view of a duct-like structure demonstrating morphological evidence of cell polarity, cell-cell junctions and an apoptotic cell within the lumen (arrow), 1000X. Right three panels depict typical organoid morphologies observed with vector control pCGN-2-P cells. Upper right panel shows duct-like structure with partial cavitation, 400X. Middle right panel shows hollowed duct-like structure, 400X and lower right panel shows high magnification view of duct-like structure, 1000X. Size bar in 400X photos equals 25  $\mu\text{m}$  and in 1000X photos equals 10  $\mu\text{m}$ .

**Fig 12. ESX-P, Ets-2-P and V12Ras-P cells form solid tumor-like structures and fail to organize into mammary gland-like structures in 3D culture.** ESX-P, Ets-2-P and V12Ras-P cells were cultured and processed as described in Fig. 11. Top panel and three left panels depict typical solid tumor-like organoids formed by ESX-P, Ets-2-P and V12Ras-P cells at 24 hr respectively, 400X. Right three panels show evidence of epithelial to mesenchymal transition in ESX-P, Ets-2-P and V12Ras-P cells at periphery of organoids after 72 hr in culture. Arrowheads identify invasive, fibroblast-like cells that penetrate into surrounding matrices. Size bar in 400X photos equals 25  $\mu\text{m}$  and in 1000X photos equals 10  $\mu\text{m}$ .

**Fig 13. Proliferative indices of cells in 3D culture demonstrate that ESX-P, Ets-2-P and V12Ras-P cells have lower mitotic rate than vector control pCGN2-P cells.** Proliferative index was determining by quantifying BrdU incorporation between 72 and 96 hr post plating, as

described in Materials and Methods. Experimental conditions were each performed in quadruplicate, and entire experiment in duplicate. Data are expressed as mean percentage of positive cells  $\pm$  SEM. Asterisk indicates statistically different from vector control cells,  $p < 0.01$ , Poisson regression, adjusted for multiple comparisons.

**Fig 14. Immunohistochemical detection of BrdU of pCGN2-P, ESX-P, Ets-2-P and V12Ras-P cells in 3D culture.** pCGN2-P, ESX-P, Ets-2-P and V12Ras-P cells were overlaid onto thick reconstituted basement membrane as single cell suspensions. After 72 hr in culture, cells were treated with 1mM BrdU for 24 hr. pCGN2-P cells (upper left) form numerous small duct-like structures (asterisk) with frequent brown staining, BrdU-positive cells (arrow). ESX-P (upper right), Ets-2-P (lower, left) and V12Ras-P (lower right) cells form disorganized, solid tumor-like organoids with few BrdU-positive cells (arrows). Invasive cells are observed to penetrate surrounding matrices (arrowheads). Experimental conditions were each performed in quadruplicate, and entire experiment in duplicate. Size bar equals 25  $\mu$ m.

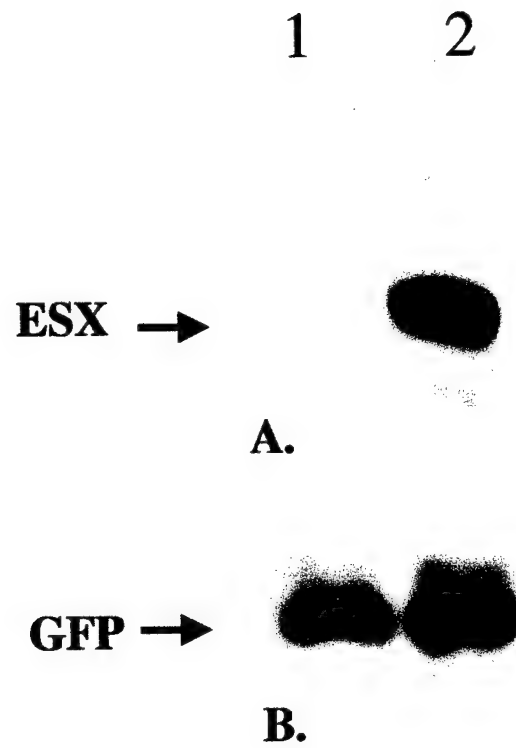


Fig 1

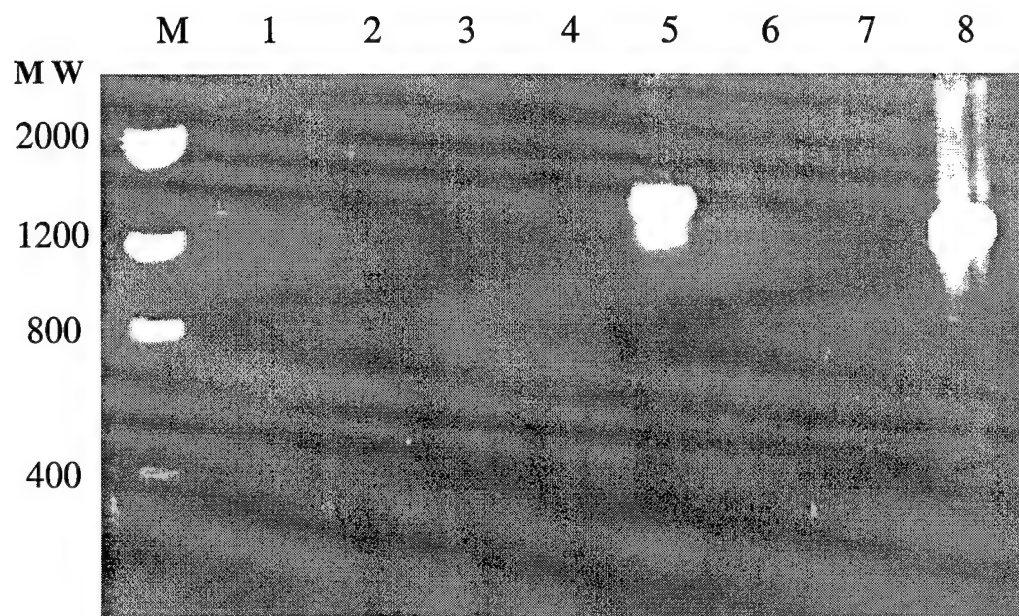


Fig 2

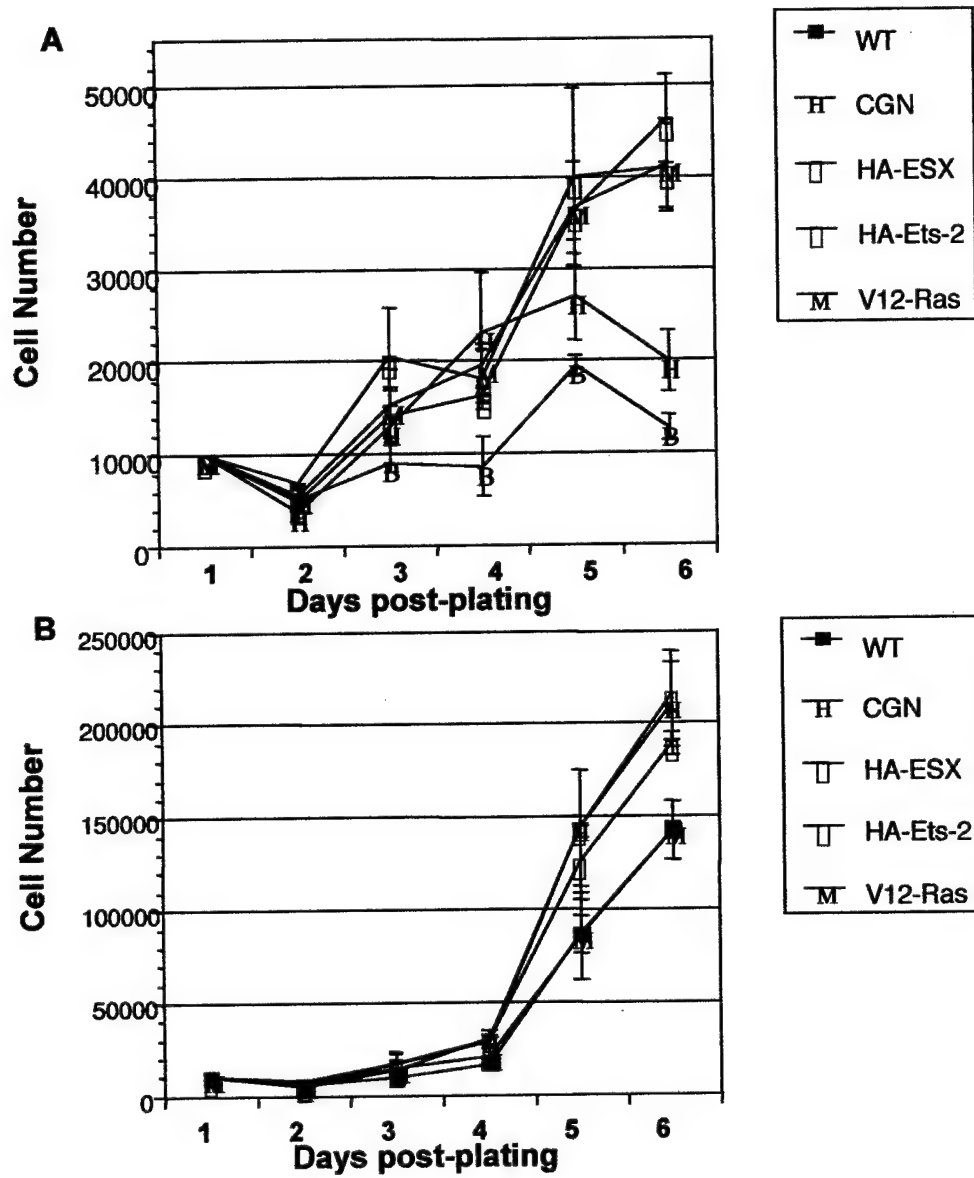


Fig 3

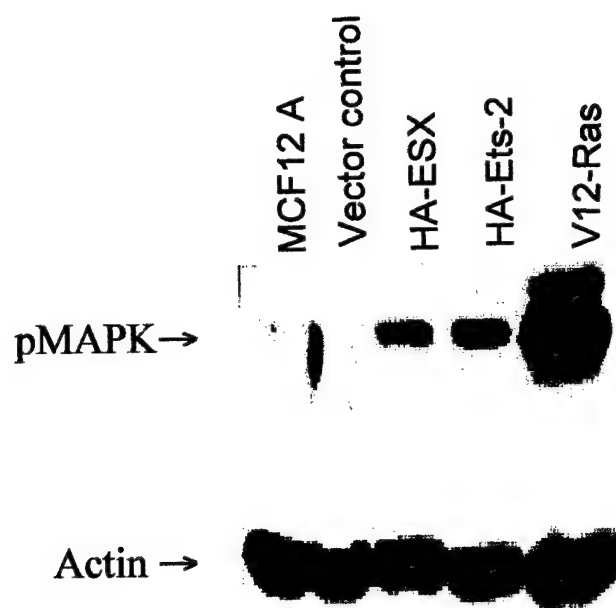


Fig 4

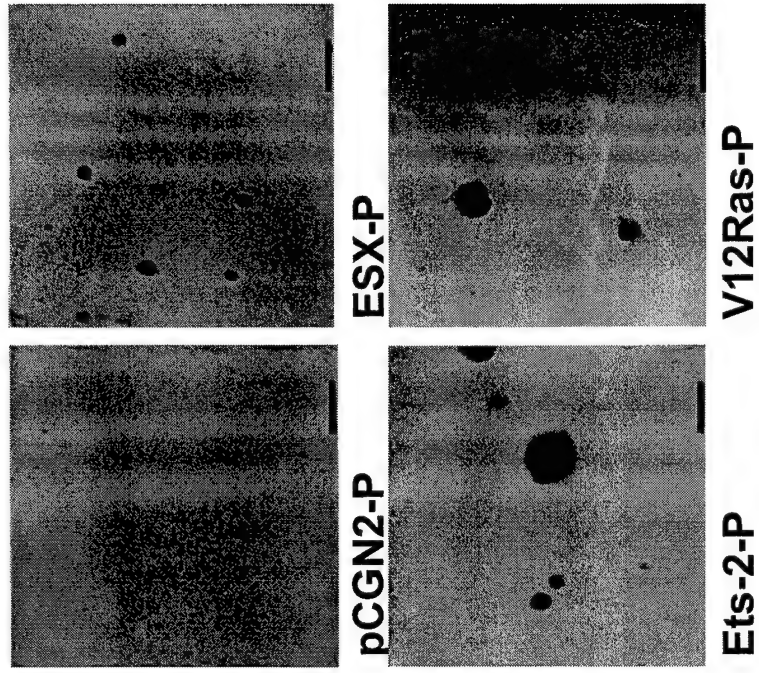


Fig 5

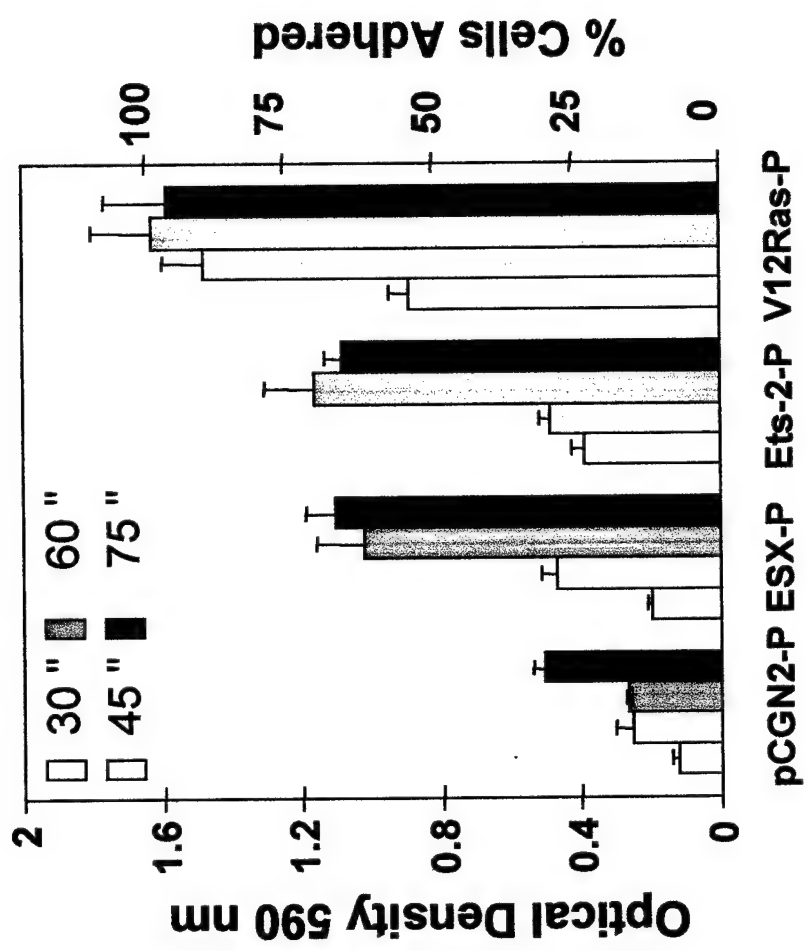


Fig 6

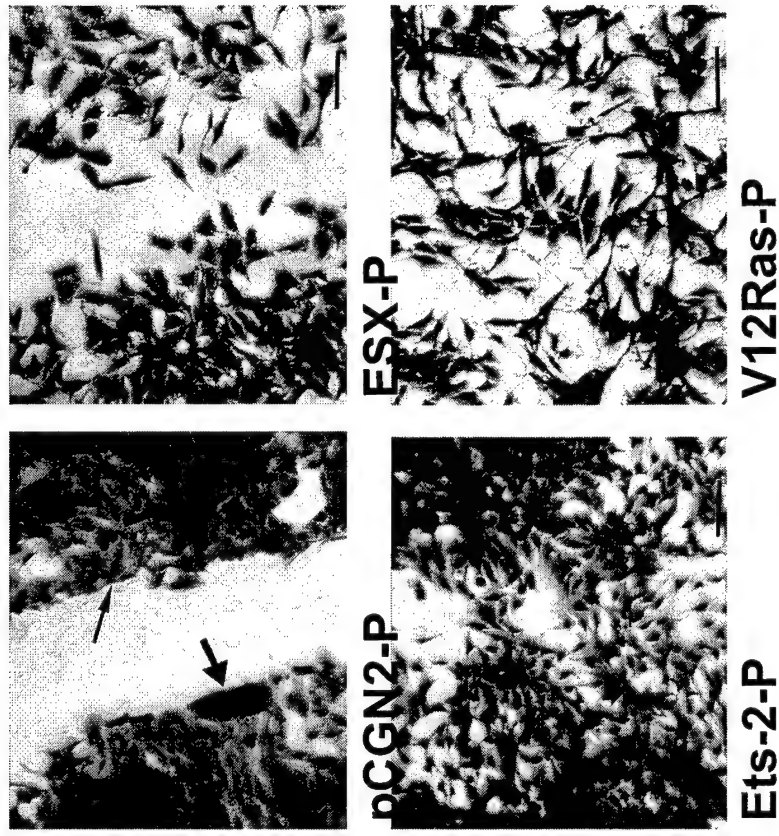


Fig 7

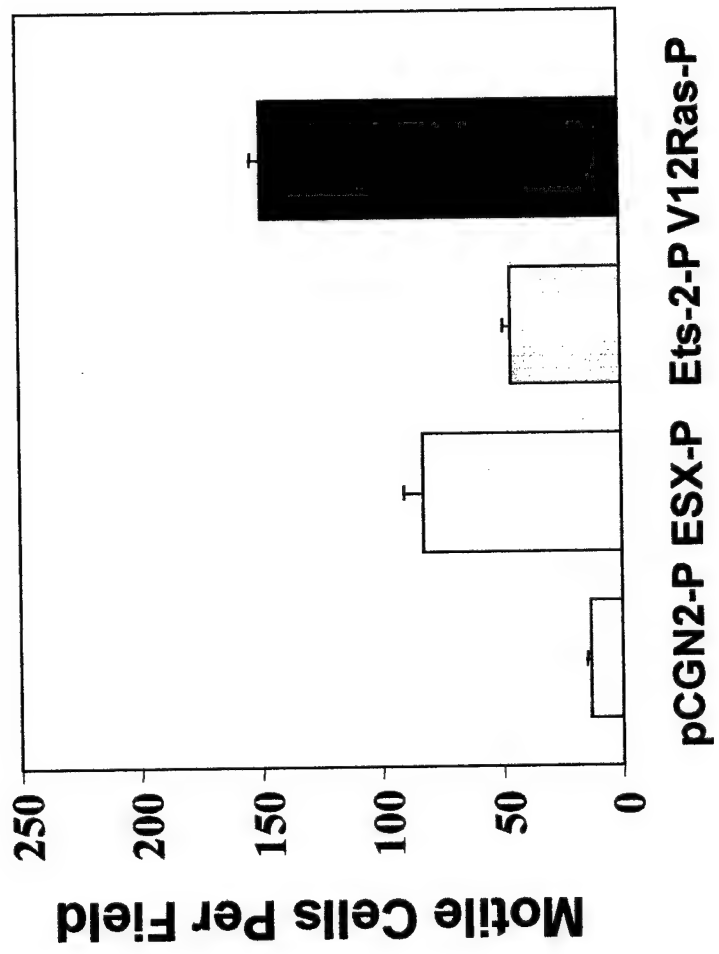


Fig 8

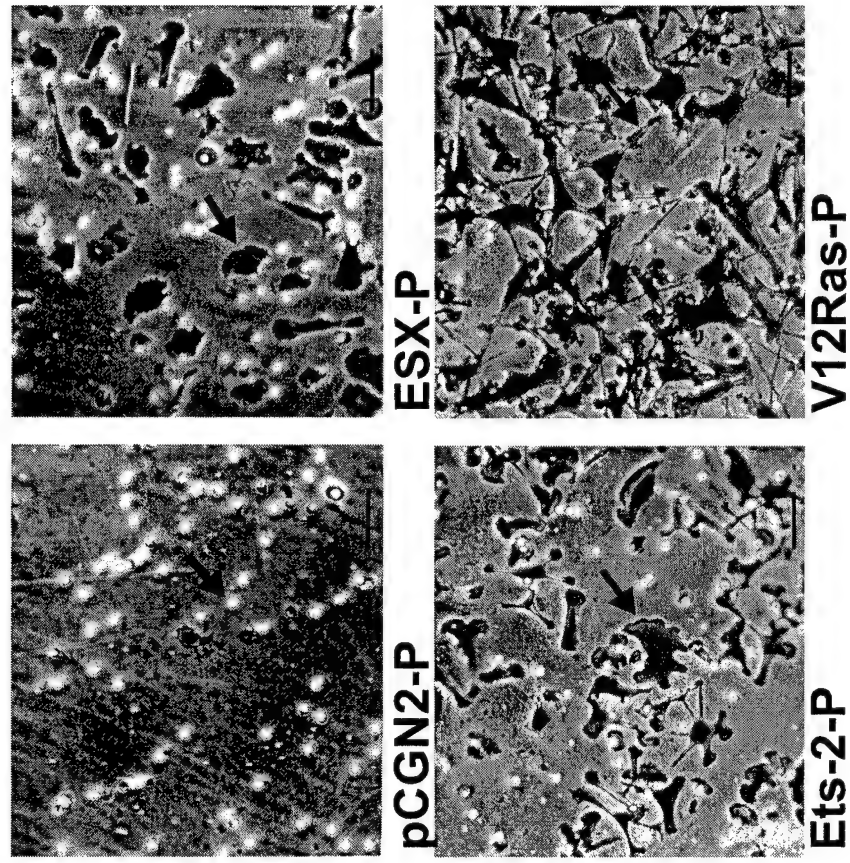


Fig 9

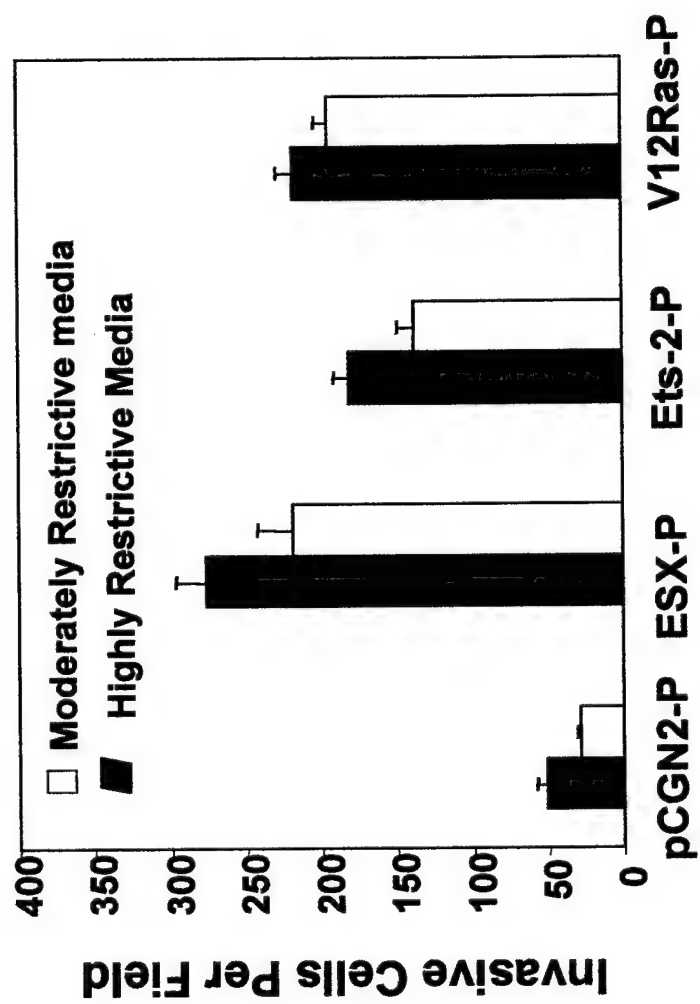


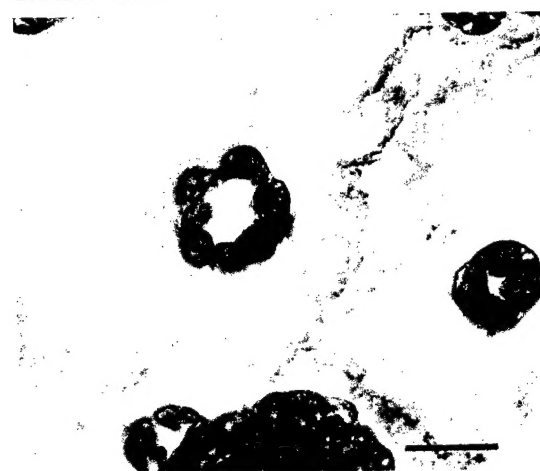
Fig 10



**MCF-12A**



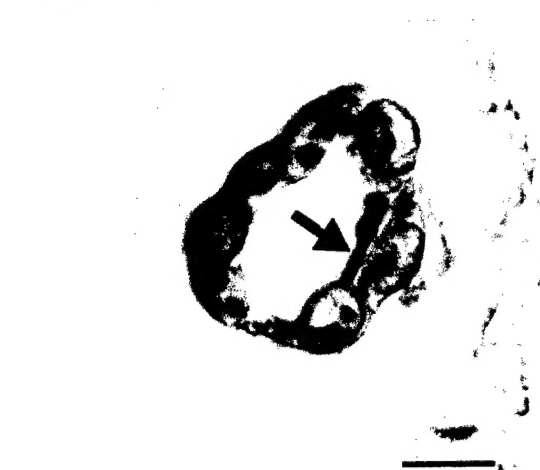
**pCGN2-P**



**MCF-12A**



**pCGN2-P**

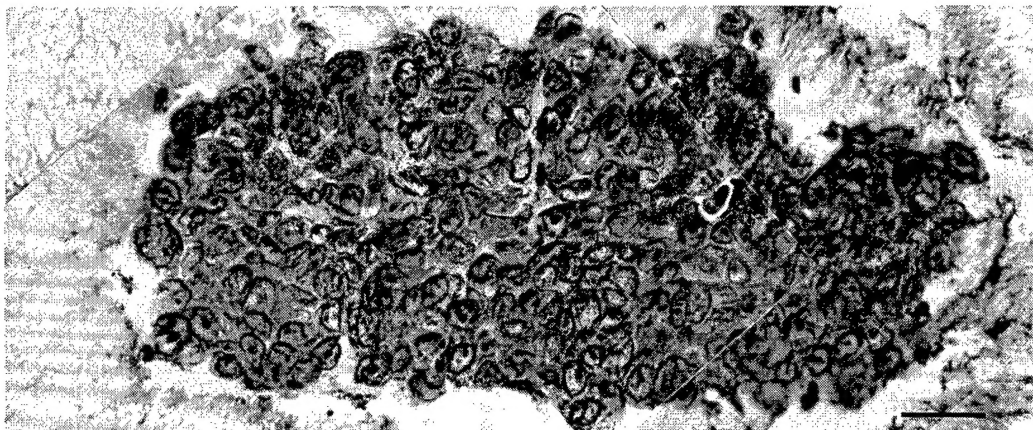


**MCF-12A**

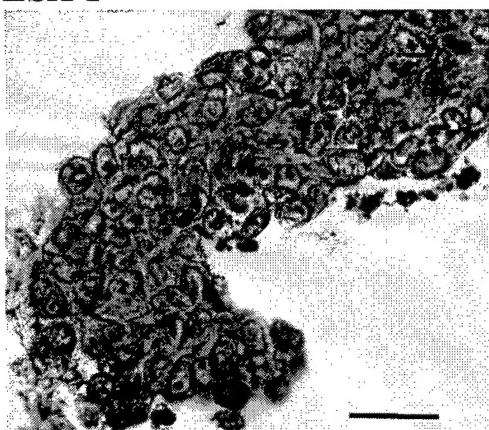


**pCGN2-P**

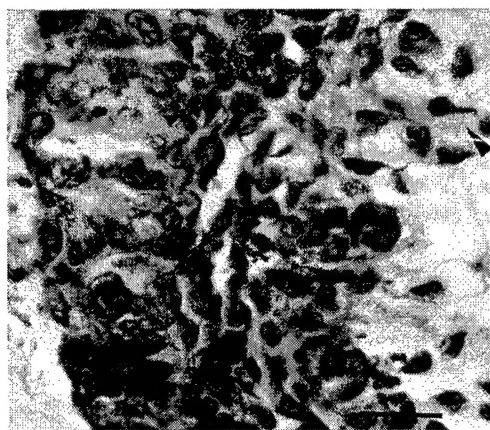
**Fig 11**



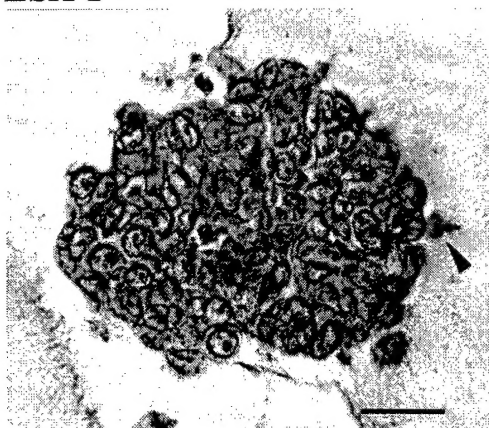
**ESX-P**



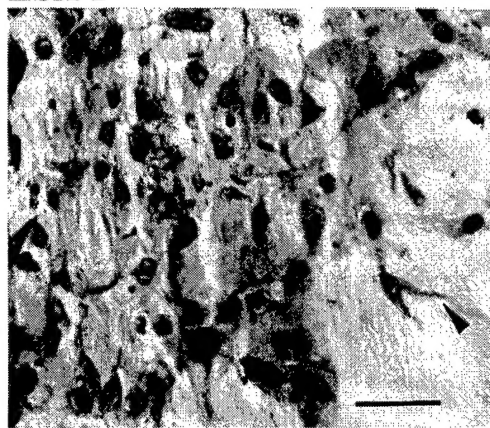
**ESX-P**



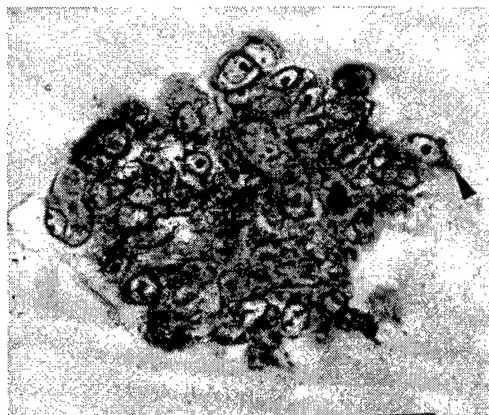
**ESX-P**



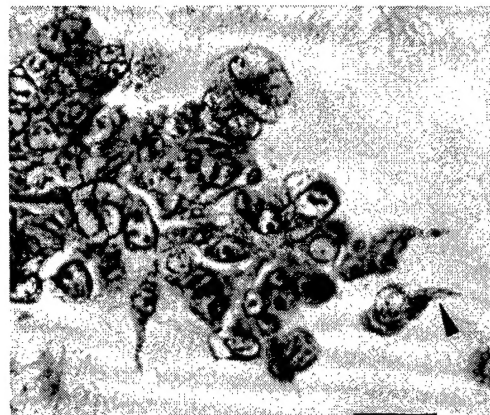
**Ets-2-P**



**Ets-2-P**



**V12Ras-P**



**V12Ras-P**

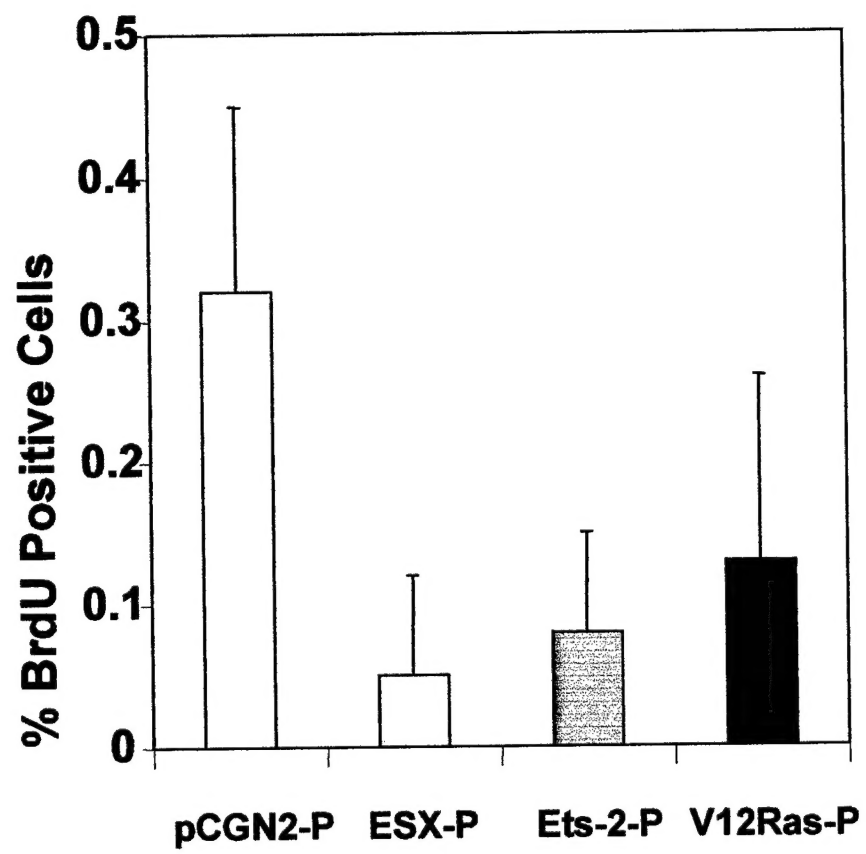
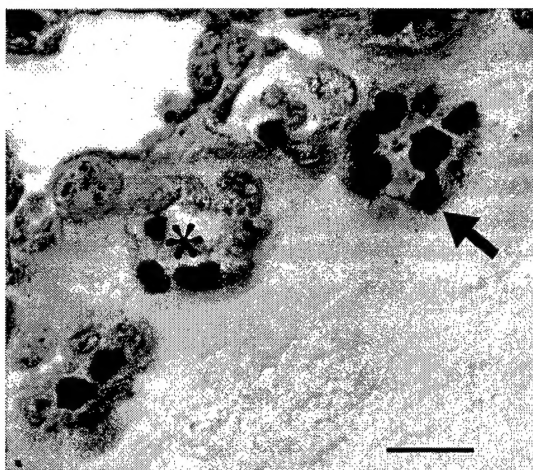
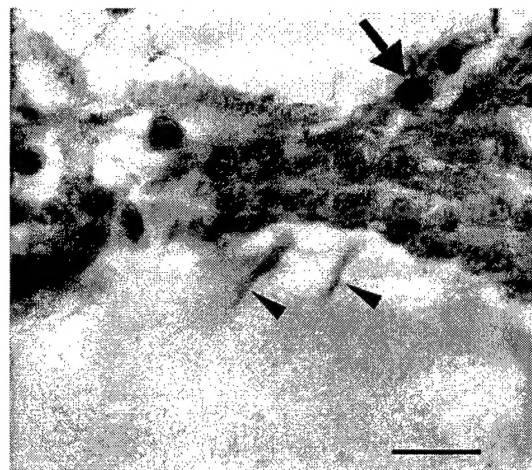


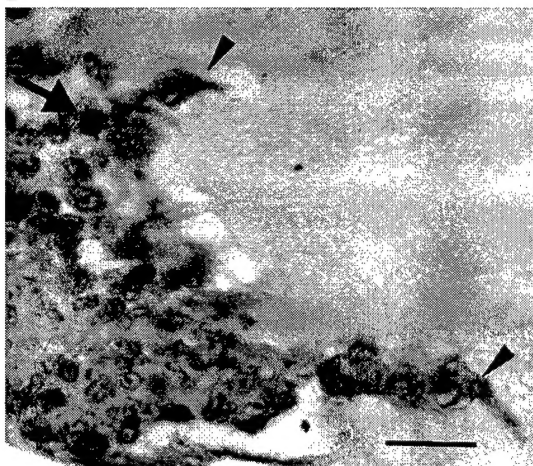
Fig 13



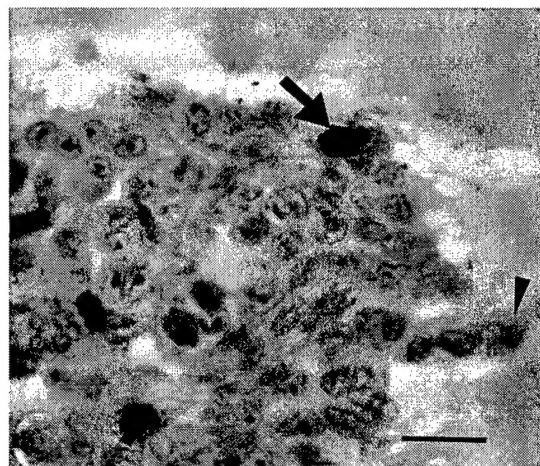
**pCGN2-P**



**ESX-P**



**Ets-2-P**



**V12Ras-P**